

國立臺灣大學醫學院解剖學暨細胞生物學研究所

博士論文

Graduate Institute of Anatomy and Cell Biology

College of Medicine

National Taiwan University

Doctoral Dissertation



B4GALT1 調節基質-整合素相互作用以控制肝細胞癌轉移
B4GALT1 regulates the extracellular matrix-integrin interaction
to control metastasis of hepatocellular carcinoma

陳柏達

Po-Da Chen

指導教授：黃敏銓 博士，吳耀銘 醫師

Advisor: Min-Chuan Huang, Ph.D. and Yao-Ming Wu, M.D.

中華民國 113 年 01 月

January 2024



誌謝

我要衷心感謝我的指導老師黃敏銓教授及吳耀銘醫師，他們在我整個學術歷程中給予了堅定的支持和指導。黃教授以其深厚的專業知識，不僅豐富了我的基礎知識，還在充滿挑戰的歲月中細緻地規劃實驗並糾正分析，不斷引導並塑造我的學習曲線。吳醫生在臨床實踐領域中形塑我臨床醫師的核心價值，引領我進入迷人的肝膽外科領域。他們的指導是我在研究和臨床生涯中的希望與指引。

謝謝實驗室資深成員，陳學亭博士和廖瑩好博士，他們的指導和補益完善了我的研究和實驗，發揮了關鍵的臨門一腳。他們及時的建議和鼓勵激勵了我，他們的見解在補充我的資料方面也至關重要。基礎實驗的領域錯綜複雜，我也多所仰賴又嘉、子琪和艾安的幫助與支持。

特別感謝我的父母，他們的理解和耐心使我能夠在臨床工作繁忙的情況下追求這條道路。對於我的弟弟，即使面臨自己臨床工作的疲勞，也替代我總是一肩擔起照顧家人的繁雜，我深表感謝。

我還要感謝這一路上的朋友和家人，他們在我每一步的旅程中與我並肩前行，提供鼓勵、支持和理解。因為與大家同行，才得以實現這段旅程。

最後，我要再次感謝老師們的堅定和支持。我能夠揮舞終點的這面旗，是因為在最艱難的時刻，老師總是點亮前方的那盞燈。

僅獻給我親愛的父親



中文摘要

Beta1,4-半乳糖轉移酶 (B4GALTs) 在各種疾病中扮演關鍵角色，包括癌症。其中，B4GALT1 在肝臟中高度表達，而患有 B4GALT1 基因突變的人通常會罹患肝病。然而，B4GALT1 對肝癌的影響長期以來一直未明確。在這項研究中，我們發現相對於相鄰的正常肝組織，肝細胞癌組織中 B4GALT1 明顯下降。此外，我們還發現低 B4GALT1 表現與肝細胞癌患者的血管侵犯性增加以及整體存活率下降有關。進一步的研究顯示，B4GALT1 的沉默或缺失增加了體外肝細胞癌細胞的遷移和侵犯性，並在小鼠中促使肺轉移。值得注意的是，我們的研究揭示了 B4GALT1 影響肝細胞癌細胞與 laminin 層黏蛋白的黏附之間的聯繫。B4GALT1 的沉默或缺失增加了細胞的黏附，而 B4GALT1 的過度表達則產生了相反的效應。通過質譜和 *Griffonia simplicifolia* 凝集素 II (GSL-II) 拉下實驗，我們確定了 integrin 整合素 $\alpha 6$ 和 $\beta 1$ 是 B4GALT1 的主要蛋白質受質，B4GALT1 通過修改它們的 N-glycan 進行調控。由於 B4GALT1 下調，導致細胞遷移和侵犯性增強，這種效應可以通過使用抗 $\alpha 6$ 或抗 $\beta 1$ 整合素的阻斷抗體明顯逆轉。這些發現表明 B4GALT1 的下調導致 N-glycan 修飾的改變，提高了整合素 $\alpha 6$ 和 $\beta 1$ 對層黏蛋白的結合能力，從而促進了肝細胞癌細胞的侵犯性。整體而言，我們的研究增加了對 B4GALT1 在肝細胞癌轉移的作用的理解，並指出針對 B4GALT1 表達下降的肝細胞癌患者，以層黏蛋白-整合素作為潛在治療策略的重要性。

關鍵詞：整合素，侵犯性，醣基化反應



Abstract

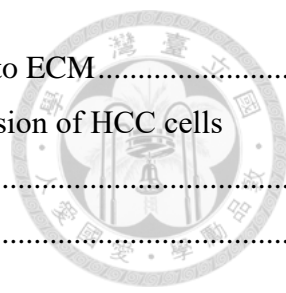
Beta-1,4-galactosyltransferases, particularly B4GALT1, are crucial enzymes implicated in various diseases, including cancer. B4GALT1's high expression in the liver and its association with liver diseases is established, but its role in liver cancer has been uncertain. This investigation reveals that B4GALT1 is significantly underexpressed in hepatocellular carcinoma (HCC) compared to non-cancerous liver tissue. This downregulation correlates with more pronounced vascular invasion and a poorer overall survival rate for those affected by HCC. Experimentally, B4GALT1 inhibition or elimination heightened HCC cell migratory and invasive behavior in vitro, and also increased the occurrence of lung metastases in animal models. Furthermore, B4GALT1 was found to be intricately linked to cell adhesion to laminin; reductions in B4GALT1 facilitated cellular adhesion, while its overexpression reduced it. Integrins $\alpha 6$ and $\beta 1$ were pinpointed as primary substrates altered by B4GALT1 via N-glycosylation, a process discernible through mass spectrometry and lectin pull-down assays. Counteracting the effects of reduced B4GALT1 on cell movement and invasiveness was possible by employing antibodies against integrins $\alpha 6$ or $\beta 1$. Overall, the study posits that diminished B4GALT1 expression contributes to the invasive potential of HCC cells by affecting the N-glycosylation and hence the binding dynamics of integrin-laminin. Consequently, this research not only advances our understanding of B4GALT1's role in HCC metastasis but also highlights targeting integrin-laminin interactions as a promising therapeutic avenue for HCC patients with low B4GALT1 expression.

Keywords: integrin, invasion, glycosylation

目 錄



口試委員會審定書.....	i
誌謝.....	ii
中文摘要.....	iii
Abstract.....	iv
List of Figures.....	vii
List of Tables.....	viii
Chapter 1. Introduction.....	1
1.1 Current predicament of hepatocellular carcinoma.....	1
1.2 The role of extracellular matrix in hepatocellular carcinoma.....	1
1.3 Abnormal glycosylation and B4GALT1 in hepatocellular carcinoma.....	2
Chapter 2. Materials and Methods.....	4
2.1 Clinical samples.....	4
2.2 Immunohistochemistry (IHC).....	4
2.3 Cell lines and cell culture.....	5
2.4 Transfection and plasmid construction.....	6
2.5 Utilizing CRISPR/Cas9 system to knockout B4GALT1 knockout in PLC5 cells.....	7
2.6 Mass spectrometric analysis.....	8
2.7 Antibodies and reagents.....	9
2.8 Western blot analysis.....	10
2.9 Experimental NOD/SCID mice model for metastasis.....	11
2.10 MTT assay.....	12
2.11 Migration (transwell) and Invasion (Matrigel) assays.....	13
2.12 Flow cytometry.....	14
2.13 Lectin pull-down assay.....	14
2.14 Cell adhesion assay.....	15
2.15 Statistical analyses.....	16
Chapter 3. Results.....	17
3.1 Lower expression levels of B4GALT1 are associated with a decline in survival outcomes for hepatocellular carcinoma patients.....	17
3.2 B4GALT1 influences the oncogenic properties of HCC cells.....	19
3.3 B4GALT1 impacts on the metastatic progression of HCC cells in Mice Models.....	20
3.4 Systematic glycoproteomics reveals integrin β 1 and α 6 as protein targets of B4GALT1.....	21

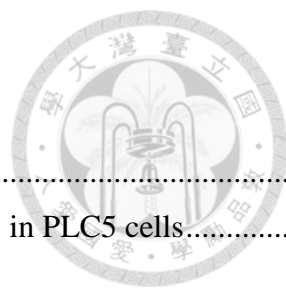


3.5 Involvement of B4GALT1 in the adhesive function of HCC Cells to ECM.....	23
3.6 Integrins $\beta 1$ and $\alpha 6$ are central to the enhanced migration and invasion of HCC cells prompted by the suppression or elimination of B4GALT1.	25
Chapter 4. Discussion	27
Reference	32



List of Figures

Figure 1. B4GALTs expression in human tissues.	36
Figure 2. Clinical significance of B4GALT1 expression in HCC.	37
Figure 3. B4GALT1 expression in normal and HCC tissues.	39
Figure 4. B4GALT1 expression in liver stromal cells and in various cancer cell lines.	40
Figure 5. B4GALT1 effects of HCC cells in vitro.	41
Figure 6. B4GALT1 effects on HCC cell viability.	42
Figure 7. B4GALT1 effects on HCC cells metastasis in vivo.	43
Figure 8. Effects of B4GALT1 knockout on glycophenotypes in PLC5 cells.	45
Figure 9. Flow cytometric analysis of ITGB1 and ITGA6 expression on the cell surface of HCC cells.	46
Figure 10. The role of B4GALT1 in HCC cells in overseeing the process of integrins $\alpha 6$ and $\beta 1$ glycosylation.	47
Figure 11. B4GALT1 exerts influence over the adhesion of HCC cells to laminin.	49
Figure 12. Effects of GSL II, RCA I, and VVA lectin on cell-laminin adhesion.	51
Figure 13. Effects of N-acetylglucosaminidase on cell-laminin adhesion and GSL II binding.	52
Figure 14. The sialylation patterns within ITGB1 and ITGA6 in PLC5 cells following the knockout of B4GALT1.	53
Figure 15. Blockade of integrin $\beta 1$ or integrin $\alpha 6$ impedes the migration and invasion promoted by B4GALT1 knockdown or knockout in HCC cells.	54
Figure 16. Representative images of HCC cell migration and invasion blocked with an anti-integrin $\beta 1$ or anti-integrin $\alpha 6$ antibody.	56
Figure 17. B4GALT1 knockdown does not significantly change levels of phospho-RTKs.	57
Figure 18. A diagrammatic illustration portraying the conceptualized mechanism by which B4GALT1 regulates HCC invasiveness.	58



List of Tables

Table 1. Correlation of B4GALT1 intensity and clinicopathologic features.	59
Table 2. Glycoproteomic analysis reveals potential substrates of B4GALT1 in PLC5 cells.....	60



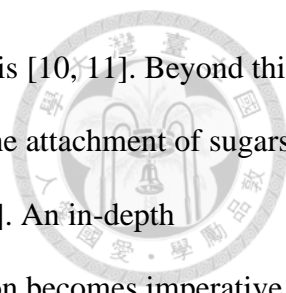
Chapter 1. Introduction

1.1 Current predicament of hepatocellular carcinoma

Hepatocellular carcinoma (HCC), an imposing global health challenge, ranks prominently as one of the most prevalent and lethal forms of cancer, constituting the primary cause of mortality associated with liver cancers [1]. The formidable mortality rate linked to HCC stems from the unfortunate circumstance of late-stage detection, where the cancer has typically advanced or infiltrated blood vessels by the time of diagnosis [2]. Compounding the challenge, an alarming 80% of HCC patients find themselves ineligible for potentially curative treatments, adding complexity to the management of this disease [3]. In the ongoing pursuit of novel prognostic models, the presence of vascular invasion emerges as a critical criterion, serving as a linchpin for predicting both the intraliver dissemination of cancer and the ominous risk of metastasis to distant anatomical sites [4, 5]. The profound role played by vascular invasion in cancer progression underscores the compelling need for an exhaustive exploration of the intricate mechanisms guiding how HCC cells breach the extracellular matrix (ECM), a pivotal step in the intricate metastatic cascade [6].

1.2 The role of extracellular matrix in hepatocellular carcinoma

The progression of HCC unfurls against the backdrop of substantial alterations in the extracellular matrix (ECM) of the tumor microenvironment [7]. Integrins, standing as the primary receptors orchestrating cell-ECM interactions, play a central role in this transformative journey. Significantly, HCC tissues exhibit an upregulation of various integrins and ECM proteins, setting them apart from their normal liver counterparts [8, 9]. This heightened expression assumes critical significance in orchestrating the chemotactic responses of HCC

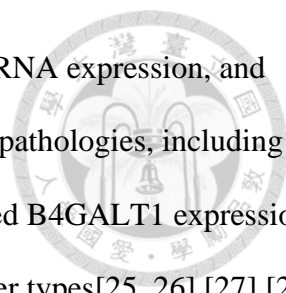


cells, aligning with their aggressive behavior and unfavorable prognosis [10, 11]. Beyond this, glycosylation, the intricately regulated enzymatic process governing the attachment of sugars to proteins, emerges as a key player in modulating integrin functions [12]. An in-depth comprehension of the nuanced modulation of integrins by glycosylation becomes imperative for the formulation of targeted therapeutic interventions against integrin-mediated cancer progression.

1.3 Abnormal glycosylation and B4GALT1 in hepatocellular carcinoma

A burgeoning body of scientific evidence establishes a compelling link between irregular oligosaccharide expression and HCC [13, 14]. The subtleties of glycan formation, encompassing initiation, extension, and branching, are pivotal for maintaining cellular function, and any disturbances in these processes are implicated in the intricate tapestry of cancer development [15, 16]. Deregulated glycosylation, with its potential to alter the interactions between cancer cells and their microenvironment, not only encourages invasive behaviors but also serves as a predictive marker for metastasis and patient survival in clinical settings [17]. The Beta-1,4-galactosyltransferases (B4GALTs) enzyme family, renowned for their conserved role in synthesizing beta-1,4-galactose linkages on N-acetylglucosamine substrates, assumes a central role in generating a diverse array of glycan structures pivotal for processes such as protein structuring, pathogen defense, immune reactions, growth factor activity, and cell adhesion [18] [19].

Among these enzymes, the significance of B4GALT1 is underscored by its pivotal role in N-glycan galactosylation [20]. Mouse knockout studies have provided invaluable insights, revealing that the absence of B4galt1 results in severe phenotypic consequences, including early mortality and impaired growth, coupled with heightened platelet adhesion to $\beta 1$ integrin



ligands [21] [22]. In humans, the liver displays elevated B4GALT1 mRNA expression, and mutations within the B4GALT1 gene have been implicated in various pathologies, including liver diseases and coagulation disorders[23] [24]. Moreover, heightened B4GALT1 expression has been correlated with diminished survival rates across diverse cancer types[25, 26] [27] [28] [29] [30]. Nevertheless, the precise functional implications of galactosylation and the augmented expression of B4GALT1 in the liver, specifically in the context of HCC, remain inadequately understood, presenting a significant lacuna in our comprehension of liver cancer pathology and offering a fertile ground for the exploration of potential therapeutic avenues.



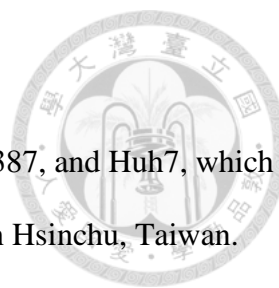
Chapter 2. Materials and Methods

2.1 *Clinical samples*

The HCC samples analyzed in this study were collected from a cohort of 78 patients at NTUH hospital between 2005 and 2010. All procedures followed were in accordance with the ethical standards of the Declaration of Helsinki and received the necessary approval from the hospital's Institutional Review Board (Approval No. 201712206RINC). Written informed consent was obtained from every patient involved, ensuring voluntary participation and confidentiality. For a comprehensive overview of the patient demographics and clinical characteristics, refer to Table 1 in the study documentation.

2.2 *Immunohistochemistry (IHC)*

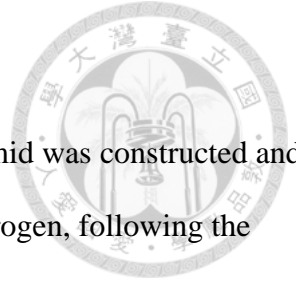
The collected tissue samples were processed by incubating them with a B4GALT1 polyclonal antibody at a dilution of 1:100 (sourced from Abnova, Taipei, Taiwan) in a controlled environment at 4 °C for a duration of 16 hours. Following this, the presence of the B4GALT1 protein was identified using the UltraVision Quanto Detection System provided by Thermo Scientific, Cheshire, UK. To ensure an unbiased evaluation, the immunohistochemistry (IHC) staining was assessed independently by two pathologists who were blinded to the clinical outcomes associated with the patients from whom the tissues were obtained.



2.3 Cell lines and cell culture

The HCC cell lines used in this study include SKHEP1, HepG2, SNU387, and Huh7, which were acquired from the Bioresource Collection and Research Center in Hsinchu, Taiwan.

Additionally, the Hep3B, HA22T, and PLC5 cell lines were obtained from the American Type Culture Collection in Manassas, VA, USA. Each cell line is identified by a specific Research Resource Identifier (RRID) to ensure traceability and reproducibility (SKHEP1: CVCL_0525, HepG2: CVCL_0027, SNU387: CVCL_0250, Huh7: CVCL_0336, Hep3B: CVCL_0326, HA22T: CVCL_7046, and PLC5: CVCL_0485). These cell lines were all cultured in Dulbecco's Modified Eagle Medium (DMEM), sourced from Thermo Fisher Scientific in Grand Island, NY, USA. The culture medium was enriched with 10% Fetal Bovine Serum (FBS), also from Thermo Fisher Scientific, along with 100 IU/mL of penicillin and 100 µg/mL of streptomycin to prevent bacterial contamination. The cell cultures were kept in a controlled environment inside a humidified incubator at 37 °C and 5% CO₂ to ensure optimal growth conditions. To guarantee the integrity and reliability of the experimental results, all human cell lines underwent authentication via short tandem repeat profiling within the last three years. Additionally, stringent testing confirmed the absence of mycoplasma in all cell cultures, thus maintaining the cells in a state suitable for research purposes.



2.4 Transfection and plasmid construction

To induce B4GALT1 overexpression, the pcDNA3.1/B4GALT1 plasmid was constructed and introduced into cells using the Lipofectamine 3000 reagent from Invitrogen, following the manufacturer's guidelines. The control for these experiments was the pcDNA3.1/myc-His plasmid, also sourced from Invitrogen. The presence and correct sequence of the insert in the plasmid were confirmed by DNA sequencing.

For the temporary reduction of B4GALT1, three specific siRNA oligonucleotides were designed to target B4GALT1, alongside medium GC content siRNAs serving as the negative control, all synthesized by Invitrogen. The sequences of siRNAs targeting B4GALT1 were as follows:

si-B4GALT1-1: 5' -GAGGCAUGUCUAUAUCUCGCCCAA-3'

si-B4GALT1-2: 5' -GAAGGACUAUGACUACACCUUGCUUU-3'

si-B4GALT1-3: 5' -CAACAGUUUCUAACCAUCA AUGGAU-3'

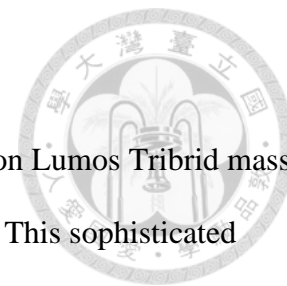
For silencing B4GALT1, cells were transfected with 20 nmol of the siRNA using Lipofectamine RNAiMAX reagent, and the silencing effect was maintained for two days. For a long-term reduction of B4GALT1, the shB4GALT1/pLKO plasmid (TRCN34839) and a non-targeting control pLKO plasmid (TRC025) were obtained from the National RNAi Core Facility at Academia Sinica in Taipei, Taiwan. The shRNA plasmids were transfected into the cells for 48 hours, after which cells were selected with 500 ng/mL puromycin for 10 days. The effectiveness and persistence of the B4GALT1 knockdown were then validated by western blotting.

2.5 Utilizing CRISPR/Cas9 system to knockout B4GALT1 knockout in PLC5 cells

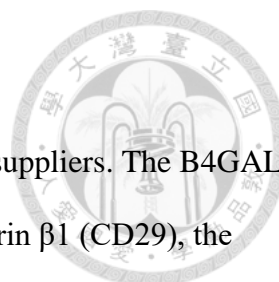
The CRISPR/Cas9 genome editing technology was utilized to create a B4GALT1 knockout in PLC5 cells. A small guide RNA (sgRNA) was designed to specifically target the B4GALT1 gene, with the sgRNA sequence determined using the predictive tools available at the CRISPR database (<http://crispr.mit.edu>). The chosen target sequence for sgB4GALT1 was: 5'

-CCTGTACGCATTATGGTCATTCA-3' . After the CRISPR/Cas9 system had been applied to the cells, the knockout of the B4GALT1 gene was confirmed by DNA sequencing to ensure the precise alteration of the genomic DNA.

2.6 Mass spectrometric analysis




LC-MS/MS analysis was conducted using the high-end Orbitrap Fusion Lumos Tribrid mass spectrometer from Thermo Fisher Scientific, located in San Jose, CA. This sophisticated instrument combines quadrupole, ion trap, and Orbitrap mass analyzers. The peptide samples were separated on the Ultimate system 3000 nanoLC, also by Thermo Fisher Scientific, situated in Bremen, Germany, which interfaced with the mass spectrometer. The peptides were loaded onto a C18 Acclaim PepMap NanoLC column, 75 μm in diameter and 25 cm in length, packed with 2 μm beads with 100 \AA pores. The liquid chromatography utilized two solvents for the mobile phase: 0.1% formic acid in water for phase A and 100% acetonitrile with 0.1% formic acid for phase B. A gradient increasing from 2% to 40% of solvent B over 50 minutes at a flow rate of 300 nL/min was used to elute the peptides. Mass spectrometry was performed in data-dependent acquisition mode. The initial full scan MS was executed at a resolution of 120,000 at $m/z=200$, setting the automatic gain control (AGC) target at $5e5$, and capping the maximum injection time at 50 milliseconds. The most intense ions were selected for high-energy collision-activated dissociation (HCD) MS/MS within a 3-second cycle. HCD-MS/MS fragmentation was done in a 1.4Da isolation window, at a resolution of 15,000, with a normalized collision energy of 32. The AGC target for MS/MS was set to $4e4$, and ions were dynamically excluded for 60 seconds post-selection. The raw MS/MS data were processed for protein identification using the Mascot and SEQUEST search algorithms within the Proteome Discoverer (PD) software suite, version 2.3 from Thermo Scientific. The search accounted for a peptide mass tolerance of 10 p.p.m. and an MS/MS ion mass tolerance of 0.02 Da. The peptide identifications were validated with a 1% false discovery rate (FDR) threshold to ensure accuracy and reliability.



2.7 Antibodies and reagents

The research utilized a range of antibodies and reagents from various suppliers. The B4GALT1 antibody was procured from Abnova (Catalog #PAB20512). For integrin $\beta 1$ (CD29), the antibody was sourced from BD Transduction Laboratories (Catalog #610468), and for integrin $\alpha 6$, it was obtained from Cell Signaling Technology Inc. (Catalog #3750). The antibody for GAPDH, a common loading control in Western blot analysis, was purchased from Meridian Life Science (Catalog #H86504M). For functional studies, blocking antibodies specific to integrin $\beta 1$ (P4C10) were acquired from Merck Millipore (Catalog #MAB1987Z), and for integrin $\alpha 6$ (CD49f), the antibodies were obtained from Invitrogen (Catalog #12-0495-82). The extracellular matrix (ECM) components used in the study included human collagen I and IV, human fibronectin, laminin, and bovine serum albumin (BSA), all of which were sourced from Sigma Aldrich (St Louis, MO, USA). Additionally, the study utilized a variety of FITC-conjugated lectins for cell surface glycan analysis, such as GSL-II-FITC, LEL-FITC, RCA-I-FITC, ECL-FITC, MAL-II-FITC, and PNA-FITC, all purchased from Vector Laboratories (Burlingame, CA, USA). These lectins are specific to different sugar moieties and are used to profile the glycosylation patterns on cell surfaces.

2.8 Western blot analysis

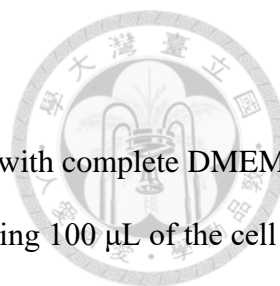


The proteins extracted from the samples were first separated by their size using SDS-PAGE (sodium dodecyl sulfate-polyacrylamide gel electrophoresis). After the separation, they were carefully transferred onto PVDF (polyvinylidene difluoride) membranes, which are commonly used for their stability and affinity for proteins. To prevent non-specific binding, the blots on the PVDF membranes were blocked with a solution containing 5% milk diluted in TBST (Tris-buffered saline, 0.1% Tween 20) for 1 hour at room temperature. This step ensures that the primary antibodies will bind only to their specific target proteins. After blocking, the membranes were incubated with the primary antibodies that target specific proteins of interest. This incubation was carried out overnight at 4 °C, allowing for a thorough and stable binding of the antibodies to the proteins. Subsequently, the blots were treated with secondary antibodies. These are antibodies that bind to the primary antibodies and are conjugated with horseradish peroxidase (HRP), an enzyme that facilitates the detection of the protein-antibody complexes. Finally, the protein bands were visualized using enhanced chemiluminescence (ECL) reagents. These reagents react with the HRP enzyme, producing a luminescent signal that can be captured on X-ray films. The intensity of the bands on the film correlates with the amount of protein present, thus providing a semi-quantitative measure of protein expression.

2.9 Experimental NOD/SCID mice model for metastasis

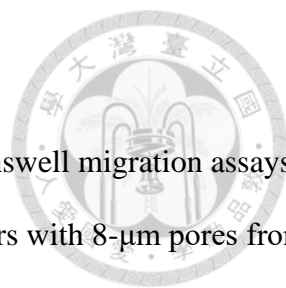
The experimental procedure for studying metastasis in NOD/SCID mice involved administering 1×10^6 HCC cells intravenously through the tail vein to 4-week-old female mice sourced from LASCO, Taipei, Taiwan. After a 60-day period, the mice were euthanized, and any metastatic nodules present were identified. Post-euthanasia, the lung tissues were preserved in paraffin for subsequent hematoxylin and eosin (H&E) staining, a standard technique for visualizing tissue structure and any pathological changes. The care and maintenance of the mice adhered to high standards, ensuring they were kept in a specific pathogen-free environment and provided with constant access to food and water, along with a stable 12-hour light/dark cycle. The ethical review and approval for this study were rigorously carried out by the Institutional Animal Care and Use Committee (IACUC) of the National Taiwan University College of Medicine, as indicated by Approval No. 20170405, ensuring that all procedures complied with established guidelines for the humane treatment and use of laboratory animals in research





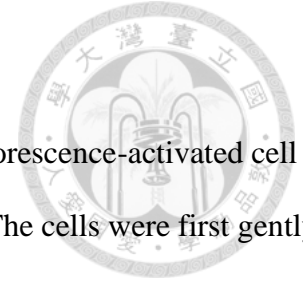
2.10 MTT assay

To assess cell viability, HCC cells were first prepared in a suspension with complete DMEM medium and then distributed into 96-well plates, with each well receiving 100 μL of the cell suspension at a concentration of 3×10^3 cells per well. To carry out the MTT assay, a widely used method to evaluate cell metabolic activity, 10 μL of an MTT solution at 5 mg/ml concentration was added to each well at predetermined intervals. The cells were incubated at 37 $^{\circ}\text{C}$ for a duration of 4 hours, allowing the MTT to be metabolized. After the incubation period, 100 μL of a 10% SDS (sodium dodecyl sulfate) solution in 0.01N HCl was added to the wells which helps to dissolve the formazan crystals formed within the cells. The absorbance of the dissolved formazan product was then measured using a spectrophotometer at two different wavelengths, 550 nm and a reference wavelength of 630 nm, to accurately determine the optical density of the solution. The difference in absorbance between these two wavelengths helps to correct for any background noise, resulting in a more precise measurement of cell viability.



2.11 Migration (transwell) and Invasion (Matrigel) assays

To measure the migratory and invasive capabilities of HCC cells, Transwell migration assays were carried out using 6.5-mm diameter polycarbonate Transwell filters with 8- μm pores from Corning Costar Corp. For the migration assay, either 3×10^4 HA22T cells or 2×10^5 PLC5 cells, suspended in 200 μL of serum-free DMEM, were seeded onto the upper compartment of the Transwell chamber. The lower compartment of 24-well plates was filled with 500 μL of DMEM supplemented with 10% FBS to act as a chemoattractant. For invasion assays, which measure the cells' ability to penetrate through an ECM-like barrier, BD PharMingen's BioCoat Matrigel invasion chambers were used. Similar to the migration assay, cells were placed in the upper compartment but had to invade through a Matrigel matrix to reach the lower chamber. After 24 hours of incubation to allow for cell migration or invasion, the cells on the underside of the Transwell filter were fixed with 100% methanol and stained with a 0.5% crystal violet solution. The number of cells that migrated or invaded was quantified by counting the stained cells under a microscope in at least three random fields per experiment, and the results were expressed as the mean \pm standard deviation. In experiments testing the role of integrins in cell migration and invasion, cells were pre-treated with 100 $\mu\text{g}/\text{ml}$ of functional blocking antibodies against integrin $\beta 1$ or integrin $\alpha 6$, or with control mouse IgG, for 30 minutes before the cells were added to the upper chamber of the Transwells. This pre-treatment was intended to inhibit the integrin function and assess its effect on the cells' ability to migrate and invade through the Transwell apparatus.




2.12 Flow cytometry

Cell surface protein expression in HCC cells was quantified using fluorescence-activated cell sorting (FACS), carried out with a cytometer from BD PharMingen. The cells were first gently detached from the culture dish using a 5 mM EDTA solution to preserve the integrity of cell surface proteins. After detachment, the cells were resuspended in a solution containing 2% BSA (bovine serum albumin) in PBS (phosphate-buffered saline) to block non-specific sites and reduce background staining. The cells were then incubated with FITC (fluorescein isothiocyanate)-conjugated lectins at a dilution of 1:100. Lectins are proteins that bind specifically to certain carbohydrate structures on the cell surface. This incubation was done on ice for 30 minutes to prevent internalization of the lectins and maintain the cells in a state suitable for analysis. Following the incubation, the cells were washed three times with ice-cold 2% BSA/PBS to remove unbound lectins and minimize non-specific fluorescence. subsequently, the fluorescence intensity was measured on a sample of 1×10^5 cells from each group using the FACS cytometer.

2.13 Lectin pull-down assay

To isolate and study glycoproteins that bind to specific lectins, cell lysates containing 1 mg of protein were incubated with biotinylated Griffonia Simplicifolia Lectin II (GSL-II) sourced from Vector Laboratories. The incubation was carried out at 4 °C for an extended period of 16 hours to ensure sufficient binding between the lectin and the glycoproteins. To capture the lectin-glycoprotein complexes, the sample was further incubated with streptavidin beads for 2 hours at room temperature to remove non-specifically bound proteins, and then the bound proteins were eluted from the beads. The eluted proteins represent the population of glycoproteins that were bound to GSL-II.

2.14 Cell adhesion assay



Cell adhesion assays are crucial for assessing the interaction between cells and various components of the ECM as previous document [17]. The concise protocol for this assay was conducted as follows: coating 96-well plates with ECM proteins—BSA (bovine serum albumin), fibronectin, laminin, collagen I, or collagen IV. Each protein was prepared at a concentration of 2.5 $\mu\text{g}/\text{mL}$ in PBS (phosphate-buffered saline) and the plates were incubated at 37 °C for 16 hours to allow for adequate coating of the wells. After the coating, the plates were blocked with 1% BSA in PBS to prevent non-specific cell adhesion. The blocking step was carried out at 37 °C for 4 hours. HCC cells were first detached from culture dishes using a 5 mM EDTA solution to preserve cell surface receptors. Detached cells were then re-suspended in serum-free DMEM. Approximately 2×10^4 cells in a volume of 100 μL were added to each coated well. The cells were allowed to adhere to the ECM-coated surface for 30 minutes in a humidified incubator set at 37 °C with 5% CO₂. After the incubation period, non-adherent cells were washed away, and the cells that had adhered to the plates were counted. An inverted microscope was used to count the adherent cells in three wells to provide an average cell adhesion level for each ECM protein coating.

2.15 Statistical analyses

The statistical analysis for the study was performed using the GraphPad Prism software, version 7. The specific statistical tests employed included Chi-Square Tests to explore the association between B4GALT1 expression levels and various clinicopathological features of HCC patients, Kaplan–Meier Method to generate survival curves, and Student's t-Test to compare the means of two groups of quantitative variables. Data in the study were presented in two formats as means \pm standard deviation (SD) for the measure of the spread or variability around the mean or as numbers and percentages for a simple count or proportion out of the total. The threshold for statistical significance was set at a p-value of less than 0.05 ($p < 0.05$).





Chapter 3. Results

3.1 Lower expression levels of B4GALT1 are associated with a decline in survival outcomes for hepatocellular carcinoma patients.

Upon examining the data from The Cancer Genome Atlas (TCGA), it was observed that B4GALT1 showed the most pronounced expression in liver tissues compared to other members of the B4GALT family (referenced in Figure 1A), with a notably higher presence in hepatic tissue than other bodily organs (referenced in Figure 1B). Contrasting these findings, the Oncomine database's Chen and Roessler liver datasets indicated a reduced presence of B4GALT1 mRNA in hepatocellular carcinoma (HCC) tissues versus normal liver tissues (referenced in Figure 2A) [31] [32]. However, a subsequent review of TCGA data disclosed a negligible difference in B4GALT1 mRNA levels when comparing normal and HCC liver tissues (referenced in Figure 3A).

Further investigations using the TCGA and Llovet-91 datasets to determine the link between B4GALT1 levels and HCC progression yielded no substantial correlations (referenced in Figure 3B). Nevertheless, survival analysis employing the Kaplan–Meier plotter and the R2 platform did suggest a connection between diminished B4GALT1 mRNA levels and decreased overall survival rates in HCC patients (referenced in Figure 2B).

Further scrutiny into B4GALT1 levels in HCC tissues, their relationship with clinical-pathological traits, and their prognostic value in HCC, was carried out.

Immunohistochemical analysis graded B4GALT1 intensity from 0 to 3, with scores of 0 and 1 indicating low levels, and 2 and 3 indicating high levels (referenced in Figure 2C). These tests corroborated a reduction of B4GALT1 in HCC tissues in comparison to neighboring non-cancerous liver tissues (referenced in Figure 2D).

Additionally, single-cell RNA sequencing data suggested the presence of B4GALT1 in both HCC and stromal cells, with a relatively lower expression in the HCC cells (referenced in

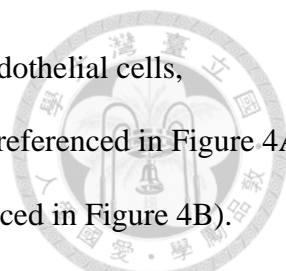


Figure 3C). It was also noted that liver stromal cells, which include endothelial cells, fibroblasts, and cholangiocytes, displayed minimal B4GALT1 levels (referenced in Figure 4A). Control IgG tests showed no specific staining in liver samples (referenced in Figure 4B). Furthermore, western blot analyses indicated the expression of B4GALT1 in HCC cell lines and in a variety of other cancer cell lines, albeit at divergent intensities (referenced in Figure 4C).

Clinicopathological analysis, which involved TNM staging by the American Joint Committee on Cancer standards, vascular invasion by microvascular invasion, and differentiation grading by the ES grading system, demonstrated that low B4GALT1 levels were frequently associated with increased vascular invasion (presented in Table 1). Additionally, Kaplan–Meier survival plots affirmed that lower B4GALT1 expression correlated with poorer overall survival ($p = 0.032$; referenced in Figure 2E). In summary, these insights highlight a significant reduction of B4GALT1 in HCC tissues compared to non-cancerous adjacent tissues and link lower B4GALT1 expression to a poorer survival prognosis in HCC patients.

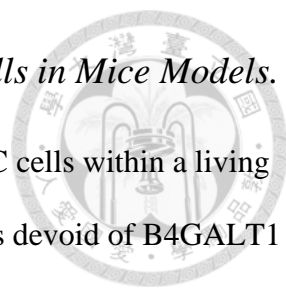
3.2 *B4GALT1 influences the oncogenic properties of HCC cells.*

In exploring B4GALT1's influence on HCC cells, we conducted a series of assays to assess cell viability, migration, and invasion in the PLC5, HA22T, and SNU387 cell lines. Utilizing MTT for viability, transwell setups for migration, and Matrigel coatings for invasion assays, we began by determining B4GALT1 levels across different HCC cell lines, observing a range of expression levels (referenced in Figure 5A). To delve deeper into B4GALT1's function, we manipulated its levels in the mentioned cell lines, both reducing and enhancing its expression. Western blot analysis confirmed these modifications (referenced in Figure 5B).

The results were intriguing; reducing B4GALT1 increased viability in HA22T cells, yet had the opposite effect on PLC5 and SNU387 cells (referenced in Figure 6). Overexpressing B4GALT1, on the other hand, didn't markedly affect the viability of PLC5 and HA22T cells, indicating a complex relationship between B4GALT1 and cell viability within different HCC cell types. Furthermore, reducing B4GALT1 expression significantly boosted the migratory and invasive capacities of all three HCC cell lines, while increasing B4GALT1 expression appeared to suppress these properties in HA22T and PLC5 cells (referenced in Figures 5C and 5D).

These findings collectively suggest that a decrease in B4GALT1 expression may contribute to the aggressive nature of HCC cells, as evidenced by the promotion of cell migration and invasion—findings that align with the earlier noted correlation between low B4GALT1 levels and increased vascular invasion in HCC.

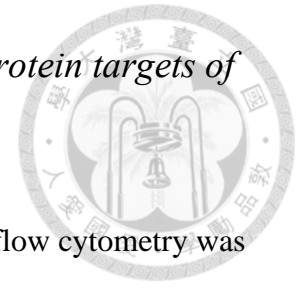
3.3 B4GALT1 impacts on the metastatic progression of HCC cells in Mice Models.



To ascertain the impact of B4GALT1 on the invasive potential of HCC cells within a living organism, we injected NOD/SCID mice intravenously with PLC5 cells devoid of B4GALT1 and HA22T cells with increased levels of B4GALT1. This allowed us to observe the formation of tumor nodules within the lungs. We utilized western blotting to validate the successful CRISPR/Cas9-mediated elimination of B4GALT1 from PLC5 cells (referenced in Figure 7A). The subsequent experiments demonstrated that the migration and invasion capacities were elevated in both clones of B4GALT1-deficient PLC5 cells (referenced in Figure 7B), consistent with prior in vitro results regarding B4GALT1-reduced PLC5 cells.

In a model designed to simulate metastasis, the absence of B4GALT1 notably increased the metastatic spread of PLC5 cells to the lungs (referenced in Figure 7C). On the flip side, augmenting B4GALT1 expression in HA22T cells had the opposite effect, restraining lung metastasis. These observations provide evidence that B4GALT1 deficiency facilitates the metastatic spread of HCC cells to the lungs, while its overexpression seems to deter such a process in a live model, supporting the hypothesis that B4GALT1's presence is inversely related to the metastatic capabilities of HCC cells.

3.4 Systematic glycoproteomics reveals integrin $\beta 1$ and $\alpha 6$ as protein targets of *B4GALT1*.



To explore B4GALT1's influence on glycophenotypes of HCC cells, flow cytometry was employed to analyze B4GALT1 knockout PLC5 cells with a variety of lectins. The knockout led to a notable increase in binding by Griffonia simplicifolia lectin II (GSL-II), as shown in Figure 8, suggesting an impact on glycosylation patterns, specifically an increased exposure of GlcNAc residues due to the absence of B4GALT1-mediated galactose addition.

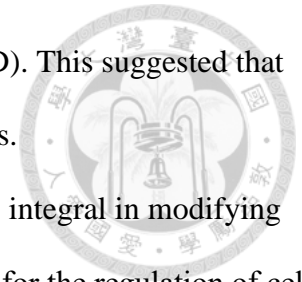
Other lectins such as LEL, RCA-I, ECL, MAL, and PNA did not show considerable binding alterations, pointing to a specific role of B4GALT1 in modifying complex-type N-glycans on cell surfaces. To pinpoint proteins that might be substrates for B4GALT1, proteins from wild-type and B4GALT1-deficient PLC5 cells were isolated using GSL-II agarose and analyzed via mass spectrometry. This analysis, detailed in Table 2, disclosed ten proteins with substantial increases in GSL-II binding, suggesting they could be substrates for B4GALT1. Notably, integrins $\beta 1$ (ITGB1) and $\alpha 6$ (ITGA6), known to be critical in cell invasion, were among these proteins [33, 34].

Further investigations, including flow cytometry, confirmed the presence of integrins $\beta 1$ and $\alpha 6$ on the surface of various HCC cell lines (referenced in Figure 9). GSL-II lectin pull-down assays corroborated the mass spectrometry results, showing increased GSL-II binding to integrins $\beta 1$ and $\alpha 6$ following B4GALT1 knockdown (referenced in Figures 10A and 10B). A significant rise in this binding post-B4GALT1 knockout implied that B4GALT1 modifies these integrins.

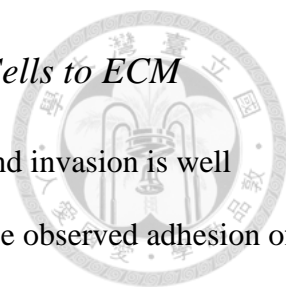
The type of glycan modifications governed by B4GALT1 was then addressed. Treatment of PLC5 cell lysates with PNGase F to remove N-glycans, followed by GSL-II lectin pull-down assays, showed a decrease in molecular weight for integrins $\beta 1$ and $\alpha 6$ and reduced GSL-II

binding post-B4GALT1 knockout (referenced in Figures 10C and 10D). This suggested that B4GALT1's actions predominantly target N-glycans on these integrins.

In summary, these findings provide strong evidence that B4GALT1 is integral in modifying N-glycans on integrins $\beta 1$ and $\alpha 6$, and these modifications are crucial for the regulation of cell invasion in HCC. This indicates that B4GALT1-mediated glycosylation alterations play a pivotal role in the invasive behavior of HCC cells.



3.5 Involvement of B4GALT1 in the adhesive function of HCC Cells to ECM

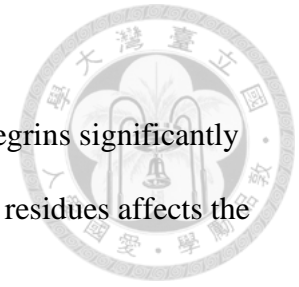


The significance of cell-ECM adhesion in controlling cell migration and invasion is well documented. To determine if B4GALT1 plays a role in this process, we observed adhesion of PLC5 cells, both with and without B4GALT1, to various ECM proteins in serum-free conditions. Notably, the absence of B4GALT1 significantly increased the adhesion of PLC5 cells to laminin, but not to collagen I, collagen IV, or fibronectin, as indicated in Figure 11A. To support the findings regarding B4GALT1's effect on laminin interaction, adhesion assays were performed with HA22T cells augmented with B4GALT1 and with B4GALT1-deficient PLC5 cells. Enhanced B4GALT1 levels led to reduced HA22T cell adhesion to laminin (Figure 11B), whereas B4GALT1 depletion resulted in stronger adhesion of PLC5 cells to laminin (Figure 11C), underlining B4GALT1's complex involvement in regulating laminin binding. Further investigation into the role of integrins $\beta 1$ and $\alpha 6$, which are crucial for laminin attachment, utilized integrin-blocking antibodies. These antibodies significantly decreased the laminin adhesion of PLC5 cells prompted by B4GALT1 knockout (Figures 11D and 11E), suggesting that B4GALT1 modulates the activity of the integrin $\alpha 6\beta 1$ complex, a prominent laminin receptor in HCC cells.

We also examined the potential function of GlcNAc in integrin-mediated cell-laminin adhesion. The adhesion assays were repeated with PLC5 cells pretreated with various lectins, and GlcNAc was enzymatically stripped from the cells using N-acetylglucosaminidase. The binding of GSL-II, which prefers GlcNAc, impeded the adhesion of B4GALT1-deficient cells to laminin but did not affect wild-type cells (Figure 12). Conversely, RCA-I, which binds to galactose residues, reduced cell-laminin adhesion, indicating a significant interaction with integrins. VVA, a lectin specific for GalNAc, however, did not show this effect. Moreover, the removal of GlcNAc lessened the adhesion of B4GALT1-knockout cells to laminin (Figure 13A). Flow cytometry analysis after the GlcNAc removal confirmed the efficiency of the

N-acetylglucosaminidase treatment (Figure 13B).

In conclusion, these experiments suggest that GlcNAc residues on integrins significantly influence cell-laminin adhesion, and B4GALT1's modulation of these residues affects the adhesive capacity of HCC cells to the ECM, especially to laminin.



3.6 Integrins $\beta 1$ and $\alpha 6$ are central to the enhanced migration and invasion of HCC cells prompted by the suppression or elimination of B4GALT1.



Integrin $\alpha 6\beta 1$ is recognized as a key laminin receptor in HCC [9]. Our findings confirm integrins $\beta 1$ and $\alpha 6$ as primary substrates of B4GALT1 in HCC cells. To examine the roles of these integrins in B4GALT1's regulatory effects on cell motility and invasiveness, HCC cells with reduced B4GALT1 levels or completely lacking B4GALT1 were treated with integrin-targeting antibodies and analyzed using migration and invasion assays (referenced in Figure 14). The use of these antibodies significantly diminished the increased cell migration and invasion usually observed following the reduction or absence of B4GALT1 in HA22T and PLC5 cells (illustrated in Figure 15A-D). These results underscore the crucial function of integrins $\beta 1$ and $\alpha 6$ in the aggressive behaviors of HCC cells induced by the downregulation of B4GALT1.

Considering the established connection between receptor tyrosine kinases (RTKs) and HCC progression [35], and our data linking B4GALT1 to the modification of the insulin receptor's glycosylation, we further explored whether B4GALT1 influences RTK activity. Our phospho-RTK array analysis, which included 58 RTKs and key signaling molecules like p-AKT and p-ERK, showed that B4GALT1 knockdown did not substantially affect their phosphorylation in PLC5 cells (presented in Figure 16). This implies that RTKs may have a limited role in the B4GALT1-mediated invasion mechanism of HCC cells, emphasizing instead the significance of integrins $\beta 1$ and $\alpha 6$.

Additional studies have indicated that sialylation can impact integrin adhesion. To investigate whether B4GALT1 absence alters sialylation patterns on ITGB1 and ITGA6, we employed lectin pull-down assays with MAL I, MAL II, and SNA. The absence of B4GALT1 did not change the sialylation of ITGB1 as evidenced by unaltered MAL II or SNA binding; however,

there was a noted decrease in MAL I binding to ITGB1, implying that B4GALT1 may influence α 2,3 sialylation on ITGB1 (as shown in Figure 17A). Contrarily, B4GALT1 did not appear to significantly impact the sialylation of ITGA6, as shown by unchanged binding of all three lectins (depicted in Figure 17B). Further investigation is necessary to solidify these observations.



Chapter 4. Discussion

Despite B4GALT1's key role as the main β 1,4-galactosyltransferase and its significant expression in the liver, its function in HCC remained ambiguous. In various cancer types, high B4GALT1 expression correlates with aggressive cancer characteristics and unfavorable patient prognosis. Our research revealed that B4GALT1 expression is reduced in HCC, correlating with vascular invasion and poorer overall patient survival rates. In line with these findings, the inhibition or absence of B4GALT1 substantially heightened HCC cell invasiveness in laboratory settings and facilitated the spread of lung metastasis in animal models. Further examinations suggested that a decrease in B4GALT1 heightened the adhesiveness of HCC cells to laminin. Integrins α 6 and β 1, components of the laminin receptor, were identified as the main proteins altered by B4GALT1, which in turn influenced the migration and invasion of cells affected by B4GALT1 suppression or deletion.

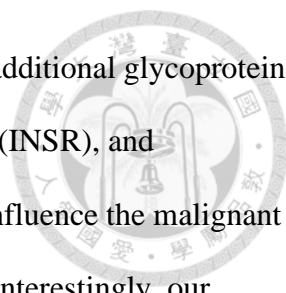
The association between the expression of B4GALT1 and cancer severity shows variation among different types of cancer. Specifically, in pancreatic cancer, elevated levels of B4GALT1 are linked with a less favorable outcome, and its overexpression is known to increase the likelihood of cancer cell spread and infiltration [27]. Similarly, in muscle-invasive bladder cancer, B4GALT1 levels serve as an indicator of a grim prognosis [26]. In contrast, glioblastomas with higher B4GALT1 expression have been associated with a longer period without disease symptoms, and reducing B4GALT1 levels in these cases has led to a rise in both cell death and autophagic processes [29]. However, our research indicates that a decrease in B4GALT1 is connected with a poorer prognosis in individuals with hepatocellular carcinoma (HCC), leading to enhanced invasion by cancer cells. The varying impacts of B4GALT1 across cancers could potentially be attributed to the interaction with different

protein substrates specific to B4GALT1.



Earlier research has suggested that in HCC, there is an upregulation of B4GALT1, which promotes the proliferation of hepatoma cells through its glycosylation functions, especially under the influence of the HBx protein from the hepatitis B virus [36]. Contrary to these findings, our study has found B4GALT1 to be less expressed in HCC, a variation that could be due to the HBV infection status of the HCC samples, given that B4GALT1 is a known target of the HBx protein. When it comes to cell proliferation, previous studies have shown that increasing B4GALT1 boosts the growth of certain liver cancer cells. Our study presents a different perspective where diminishing B4GALT1 levels led to reduced growth in some HCC cell lines while unexpectedly promoting growth in others, suggesting that B4GALT1's role in the proliferation of HCC cells is dependent on the cellular context. Moreover, our data consistently demonstrate that inhibiting B4GALT1 enhances the invasiveness of several HCC cell lines.

In our endeavor to pinpoint the protein substrates of B4GALT1, we employed GSL-II lectin pull-down assays coupled with mass spectrometry analysis. For assessing the impact of B4GALT1 elimination on the glycan structures of hepatocellular carcinoma (HCC) cells, a suite of Gal-specific lectins (LEL, RCA-I, ECL, PNA) and a GlcNAc-specific lectin (GSL-II) were utilized. The absence of B4GALT1 didn't markedly change how these lectins attached to HCC cells, except for a notable rise in GSL-II binding, indicating its utility in identifying proteins interacting with B4GALT1. Proteomics data revealed integrins $\beta 1$ and $\alpha 6$ as the primary glycoproteins affected by B4GALT1 deletion, corroborating earlier findings regarding integrin $\beta 1$ as a substrate of B4galt1 in megakaryocytes [22]. This investigation is the inaugural report of integrin $\alpha 6$ galactosylation by B4GALT1. Integrins play a crucial role in controlling



cell attachment, movement, and invasiveness [37]. Beyond integrins, additional glycoproteins such as the neutral amino acid transporter (SLC1A5), insulin receptor (INSR), and growth/differentiation factor 15 (GDF15), all of which are known to influence the malignant properties of cancer cells, were also regulated by B4GALT1 [38-40]. Interestingly, our phospho-RTK array analysis indicated that B4GALT1 suppression did not significantly impact INSR phosphorylation. However, integrins $\beta 1$ and $\alpha 6$ seem to have a crucial function in the enhanced invasiveness of HCC cells mediated by B4GALT1 suppression, as demonstrated by the ability of blocking antibodies against these integrins to mitigate the increased cell migration and invasion. This points to the significant role of integrins $\beta 1$ and $\alpha 6$ in B4GALT1-related invasiveness in HCC. Further research is needed to ascertain whether B4GALT1 affects other biological processes through these glycoproteins.

The current investigation has uncovered that the suppression of B4GALT1 enhances the adhesive, migratory, and invasive capabilities of cells interacting with laminin, which primarily relies on integrins $\beta 1$ and $\alpha 6$. It's been documented that glycosylation plays a significant part in the structural and functional integrity of integrins, with N-glycans being integral for their shape, stability, and binding abilities [41, 42]. Specifically, N-glycosylation within the I-like domain of integrin $\beta 1$ is indispensable for the assembly of heterodimers and the subunit's functional activity [43]. The suggested mechanism by which B4GALT1 suppression increases cell invasiveness involves B4GALT1 reduction causing changes in the N-glycans of integrins $\beta 1$ and $\alpha 6$. This may trigger a more engaged form of the integrin $\alpha 6\beta 1$ heterodimer, thereby bolstering cell adhesion to laminin and subsequently elevating the migration and invasiveness of HCC cells. Remarkably, B4GALT1 knockout revealed an increased exposure of GlcNAc residues on integrins, and the enzymatic removal of GlcNAc lessened cell adhesion to laminin. This suggests that GlcNAc residues are implicated in directing cell migration and invasion,

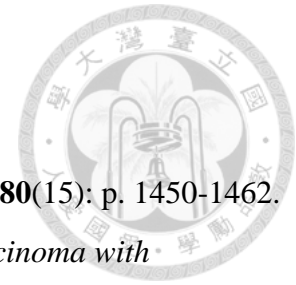
possibly through modulating integrin conformation. Earlier research has pointed to the involvement of enzymes from the N-acetylglucosaminyltransferase family in adding GlcNAc sugars onto N-glycans [44]. Thus, these enzymes could also be influencing the glycosylation and activity of integrins, and in turn, affecting cell movement and invasive behavior.

The dialogue between tumor cells and laminins through integrins that bind laminin is pivotal in the progression and spread of tumors [45]. Specifically, integrins $\alpha 6$ and $\beta 1$ show higher expression levels in hepatocellular carcinoma (HCC) than in healthy liver tissue, with the integrin $\alpha 6\beta 1$ being recognized as the key laminin receptor [9, 46, 47]. Research supports that disrupting the function of either integrin $\alpha 6$ or $\beta 1$ can diminish HCC cell invasion and the potential for metastasis [45, 47-49]. Our findings indicate that diminished B4GALT1 expression increases the migratory and invasive behavior of HCC cells; however, this effect can be countered by antibodies targeting integrin $\alpha 6$ or $\beta 1$. While drugs aimed at integrins are in the pipeline, their success in cancer treatment has been limited so far [50-52]. Hence, it's essential to find new avenues for integrin-focused therapies. Upcoming research should investigate if HCC patients with reduced B4GALT1 expression could benefit from therapies antagonizing integrin $\alpha 6$ or $\beta 1$.

The study concludes that B4GALT1 expression is reduced in HCC, and this reduction is linked with vascular invasion and adverse prognoses in patients with HCC. This is corroborated by the observation that the suppression or absence of B4GALT1 enhances the invasive capabilities of HCC cells both in lab settings and in animal models, due to alterations in N-glycan structures and integrin functions, specifically $\alpha 6$ and $\beta 1$. The findings shed light on the role of B4GALT1 in diseases influenced by integrin dynamics and propose that disrupting the interaction between laminin and integrins might be an effective approach for treating HCC characterized by low

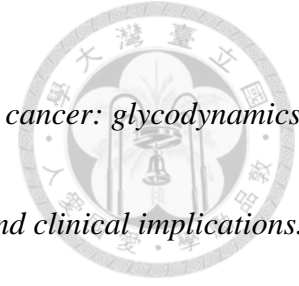
B4GALT1 levels.





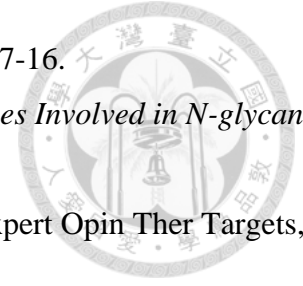
Reference

1. Villanueva, A., *Hepatocellular Carcinoma*. N Engl J Med, 2019. **380**(15): p. 1450-1462.
2. Finn, R.S., et al., *Therapies for advanced stage hepatocellular carcinoma with macrovascular invasion or metastatic disease: A systematic review and meta-analysis*. Hepatology, 2018. **67**(1): p. 422-435.
3. Reig, M., et al., *BCLC strategy for prognosis prediction and treatment recommendation: The 2022 update*. J Hepatol, 2022. **76**(3): p. 681-693.
4. Beumer, B.R., et al., *Systematic review and meta-analysis of validated prognostic models for resected hepatocellular carcinoma patients*. Eur J Surg Oncol, 2022. **48**(3): p. 492-499.
5. Zhang, X., et al., *Significance of presence of microvascular invasion in specimens obtained after surgical treatment of hepatocellular carcinoma*. J Gastroenterol Hepatol, 2018. **33**(2): p. 347-354.
6. Chen, Q., et al., *Molecular Imaging of Tumor Microenvironment to Assess the Effects of Locoregional Treatment for Hepatocellular Carcinoma*. Hepatol Commun, 2022. **6**(4): p. 652-664.
7. Zhang, J., et al., *Identifying cancer-associated fibroblasts as emerging targets for hepatocellular carcinoma*. Cell Biosci, 2020. **10**(1): p. 127.
8. Becchetti, A. and A. Arcangeli, *Integrins and ion channels in cell migration: implications for neuronal development, wound healing and metastatic spread*. Adv Exp Med Biol, 2010. **674**: p. 107-23.
9. Ozaki, I., et al., *Differential expression of laminin receptors in human hepatocellular carcinoma*. Gut, 1998. **43**(6): p. 837-42.
10. Fu, B.H., Z.Z. Wu, and C. Dong, *Integrin beta1 mediates hepatocellular carcinoma cells chemotaxis to laminin*. Hepatobiliary Pancreat Dis Int, 2004. **3**(4): p. 548-51.
11. Fu, B.H., Z.Z. Wu, and J. Qin, *Effects of integrin alpha6beta1 on migration of hepatocellular carcinoma cells*. Mol Biol Rep, 2011. **38**(5): p. 3271-6.
12. Marsico, G., et al., *Glycosylation and Integrin Regulation in Cancer*. Trends Cancer, 2018. **4**(8): p. 537-552.
13. Kang, X., et al., *Glycan-related gene expression signatures in human metastatic hepatocellular carcinoma cells*. Exp Ther Med, 2012. **3**(3): p. 415-422.
14. Kudo, T., et al., *N-glycan alterations are associated with drug resistance in human*



- hepatocellular carcinoma*. *Mol Cancer*, 2007. **6**: p. 32.
15. Brockhausen, I., *Mucin-type O-glycans in human colon and breast cancer: glycodynamics and functions*. *EMBO Rep*, 2006. **7**(6): p. 599-604.
 16. Pinho, S.S. and C.A. Reis, *Glycosylation in cancer: mechanisms and clinical implications*. *Nat Rev Cancer*, 2015. **15**(9): p. 540-55.
 17. Schjoldager, K.T., et al., *Probing isoform-specific functions of polypeptide GalNAc-transferases using zinc finger nuclease glycoengineered SimpleCells*. *Proc Natl Acad Sci U S A*, 2012. **109**(25): p. 9893-8.
 18. Qasba, P.K., B. Ramakrishnan, and E. Boeggeman, *Structure and function of beta-1,4-galactosyltransferase*. *Curr Drug Targets*, 2008. **9**(4): p. 292-309.
 19. Rodriguez, E., S.T.T. Schettters, and Y. van Kooyk, *The tumour glyco-code as a novel immune checkpoint for immunotherapy*. *Nat Rev Immunol*, 2018. **18**(3): p. 204-211.
 20. Bydlinski, N., et al., *The contributions of individual galactosyltransferases to protein specific N-glycan processing in Chinese Hamster Ovary cells*. *J Biotechnol*, 2018. **282**: p. 101-110.
 21. Chen, J., et al., *Expression of Notch signaling pathway genes in mouse embryos lacking beta4galactosyltransferase-1*. *Gene Expr Patterns*, 2006. **6**(4): p. 376-82.
 22. Giannini, S., et al., *beta4GALT1 controls beta1 integrin function to govern thrombopoiesis and hematopoietic stem cell homeostasis*. *Nat Commun*, 2020. **11**(1): p. 356.
 23. Sato, T., et al., *Molecular cloning of a human cDNA encoding beta-1,4-galactosyltransferase with 37% identity to mammalian UDP-Gal:GlcNAc beta-1,4-galactosyltransferase*. *Proc Natl Acad Sci U S A*, 1998. **95**(2): p. 472-7.
 24. Guillard, M., et al., *B4GALT1-congenital disorders of glycosylation presents as a non-neurologic glycosylation disorder with hepatointestinal involvement*. *J Pediatr*, 2011. **159**(6): p. 1041-3 e2.
 25. De Vitis, C., et al., *B4GALT1 Is a New Candidate to Maintain the Stemness of Lung Cancer Stem Cells*. *J Clin Med*, 2019. **8**(11).
 26. Xie, H., et al., *B4GALT1 expression predicts prognosis and adjuvant chemotherapy benefits in muscle-invasive bladder cancer patients*. *BMC Cancer*, 2018. **18**(1): p. 590.
 27. Chen, Y., et al., *Galactosyltransferase B4GALT1 confers chemoresistance in pancreatic ductal adenocarcinomas by upregulating N-linked glycosylation of CDK11(p110)*. *Cancer Lett*, 2021. **500**: p. 228-243.
 28. Xie, H., et al., *Increased B4GALT1 expression associates with adverse outcome in patients*

- with non-metastatic clear cell renal cell carcinoma. *Oncotarget*, 2016. **7**(22): p. 32723-30.
29. Wang, P., X. Li, and Y. Xie, *B4GalT1 Regulates Apoptosis and Autophagy of Glioblastoma In Vitro and In Vivo*. *Technol Cancer Res Treat*, 2020. **19**: p. 1533033820980104.
30. Ren, Z., et al., *High expression of B4GALT1 is associated with poor prognosis in acute myeloid leukemia*. *Front Genet*, 2022. **13**: p. 882004.
31. Chen, X., et al., *Gene expression patterns in human liver cancers*. *Mol Biol Cell*, 2002. **13**(6): p. 1929-39.
32. Roessler, S., et al., *A unique metastasis gene signature enables prediction of tumor relapse in early-stage hepatocellular carcinoma patients*. *Cancer Res*, 2010. **70**(24): p. 10202-12.
33. Huang, W., et al., *ITGBL1 promotes cell migration and invasion through stimulating the TGF-beta signalling pathway in hepatocellular carcinoma*. *Cell Prolif*, 2020. **53**(7): p. e12836.
34. Kim, Y.R., M.R. Byun, and J.W. Choi, *Integrin alpha6 as an invasiveness marker for hepatitis B viral X-driven hepatocellular carcinoma*. *Cancer Biomark*, 2018. **23**(1): p. 135-144.
35. Llovet, J.M., et al., *Molecular therapies and precision medicine for hepatocellular carcinoma*. *Nat Rev Clin Oncol*, 2018. **15**(10): p. 599-616.
36. Wei, Y., et al., *Identification of beta-1,4-galactosyltransferase I as a target gene of HBx-induced cell cycle progression of hepatoma cell*. *J Hepatol*, 2008. **49**(6): p. 1029-37.
37. Hamidi, H. and J. Ivaska, *Every step of the way: integrins in cancer progression and metastasis*. *Nat Rev Cancer*, 2018. **18**(9): p. 533-548.
38. Lin, J., et al., *SLCIA5 Silencing Inhibits Esophageal Cancer Growth via Cell Cycle Arrest and Apoptosis*. *Cell Physiol Biochem*, 2018. **48**(1): p. 397.
39. Saisana, M., S.M. Griffin, and F.E.B. May, *Insulin and the insulin receptor collaborate to promote human gastric cancer*. *Gastric Cancer*, 2022. **25**(1): p. 107-123.
40. Li, L., et al., *GDF15 knockdown suppresses cervical cancer cell migration in vitro through the TGF-beta/Smad2/3/Snail1 pathway*. *FEBS Open Bio*, 2020. **10**(12): p. 2750-2760.
41. Cai, X., et al., *The importance of N-glycosylation on beta(3) integrin ligand binding and conformational regulation*. *Sci Rep*, 2017. **7**(1): p. 4656.
42. Gu, J. and N. Taniguchi, *Regulation of integrin functions by N-glycans*. *Glycoconj J*, 2004. **21**(1-2): p. 9-15.
43. Isaji, T., et al., *N-glycosylation of the I-like domain of beta1 integrin is essential for beta1 integrin expression and biological function: identification of the minimal N-glycosylation*



- requirement for alpha5beta1. *J Biol Chem*, 2009. **284**(18): p. 12207-16.
44. Nagae, M., et al., *3D Structure and Function of Glycosyltransferases Involved in N-glycan Maturation*. *Int J Mol Sci*, 2020. **21**(2).
45. Wu, Y., et al., *Targeting integrins in hepatocellular carcinoma*. *Expert Opin Ther Targets*, 2011. **15**(4): p. 421-37.
46. Torimura, T., et al., *Coordinated expression of integrin alpha6beta1 and laminin in hepatocellular carcinoma*. *Hum Pathol*, 1997. **28**(10): p. 1131-8.
47. Fu, B.H., Z.Z. Wu, and J. Qin, *Effects of integrins on laminin chemotaxis by hepatocellular carcinoma cells*. *Mol Biol Rep*, 2010. **37**(3): p. 1665-70.
48. Lv, G., et al., *RNA interference targeting human integrin alpha6 suppresses the metastasis potential of hepatocellular carcinoma cells*. *Eur J Med Res*, 2013. **18**(1): p. 52.
49. Patman, G., *Liver: loss of integrin beta1 impairs liver regeneration and HCC progression*. *Nat Rev Gastroenterol Hepatol*, 2014. **11**(7): p. 392.
50. Hou, W., et al., *Integrin subunit beta 8 contributes to lenvatinib resistance in HCC*. *Hepatol Commun*, 2022. **6**(7): p. 1786-1802.
51. Slack, R.J., et al., *Emerging therapeutic opportunities for integrin inhibitors*. *Nat Rev Drug Discov*, 2022. **21**(1): p. 60-78.
52. Dhaliwal, D. and T.G. Shepherd, *Molecular and cellular mechanisms controlling integrin-mediated cell adhesion and tumor progression in ovarian cancer metastasis: a review*. *Clin Exp Metastasis*, 2022. **39**(2): p. 291-301.



Figures and figure legends

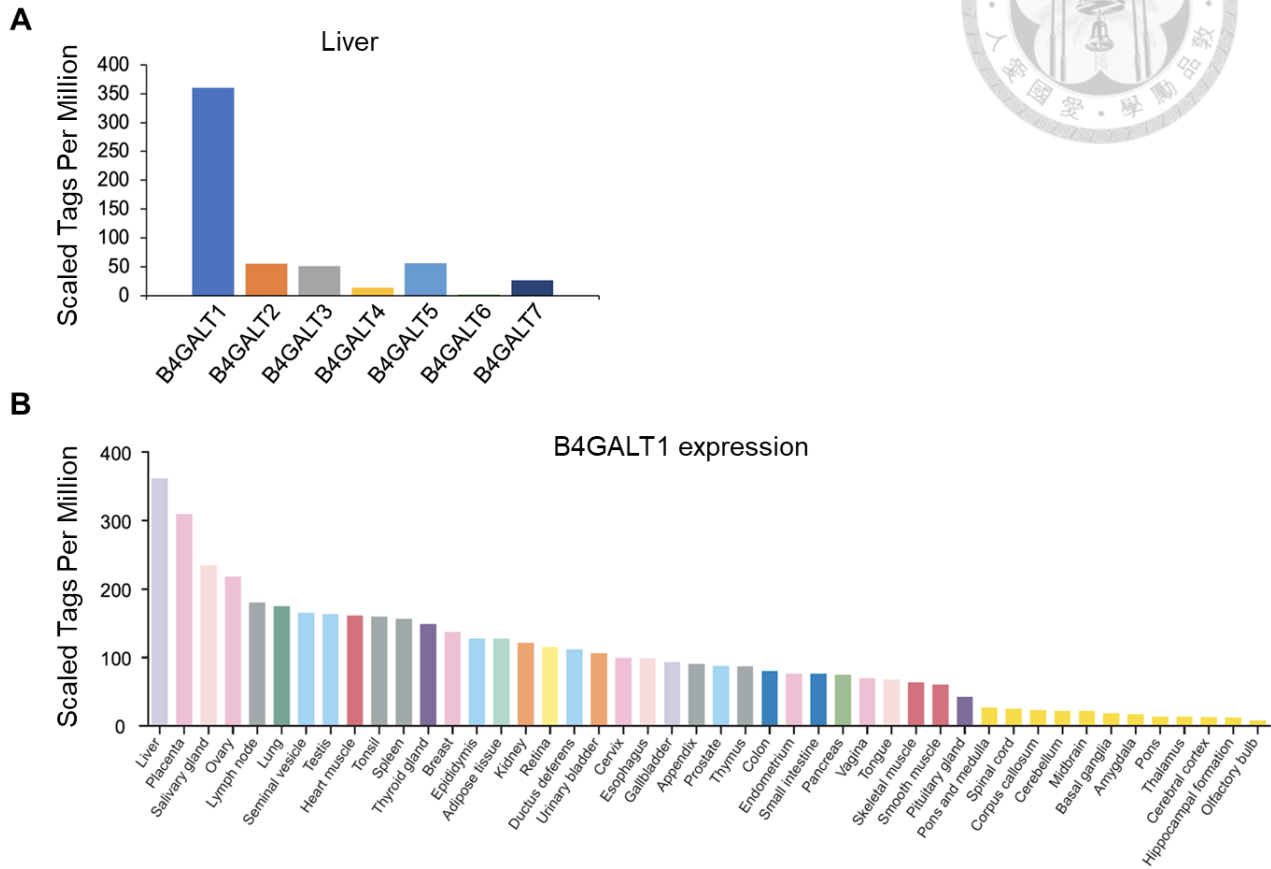


Figure 1. B4GALTs expression in human tissues.

A. Within the seven-member B4GALT gene family, B4GALT1 is the most abundantly expressed gene in the liver. **B.** Out of 46 human tissue types, B4GALT1 exhibits the highest expression levels in the liver, according to data sourced from the FANTOM5 project featured in The Human Protein Atlas (HPA).

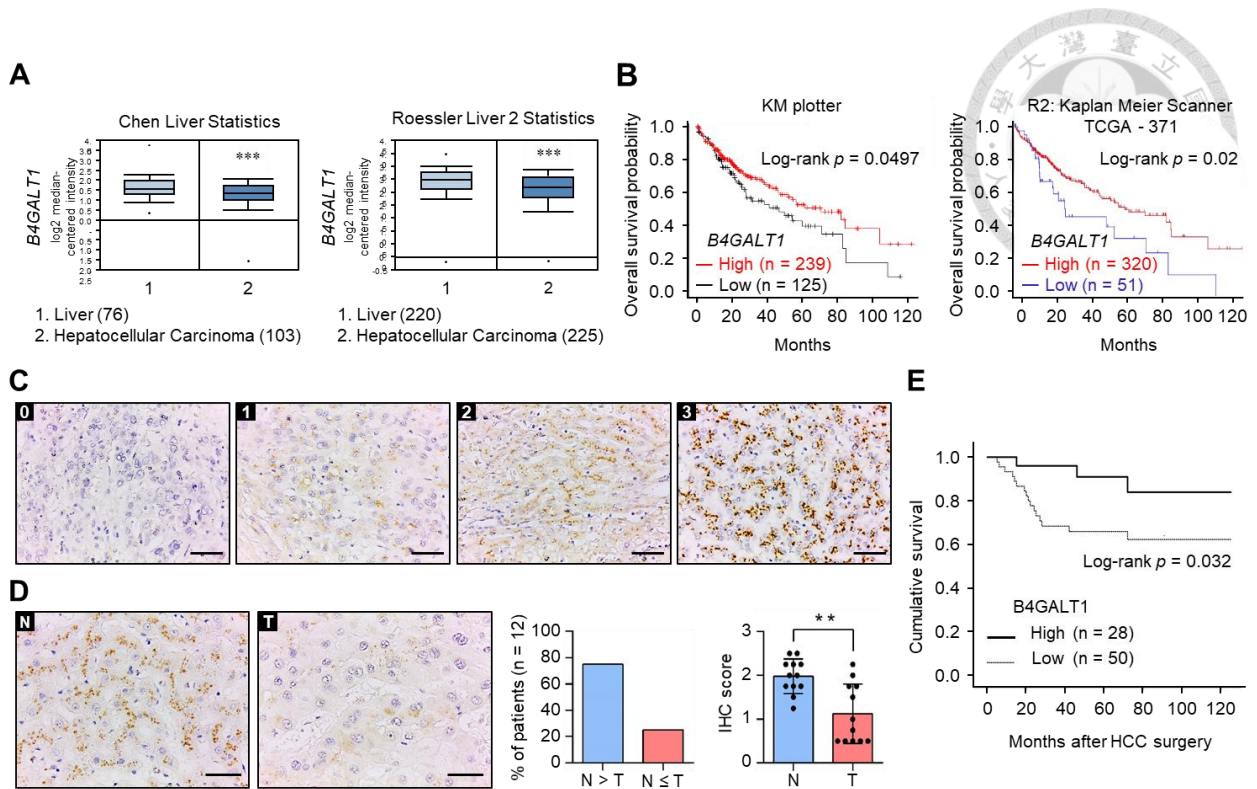
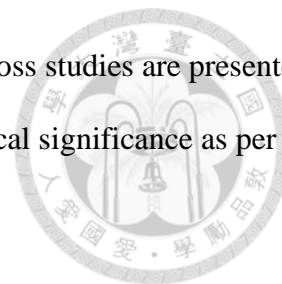


Figure 2. Clinical significance of B4GALT1 expression in HCC.

A. Oncomine database research shows a lower expression of B4GALT1 in hepatocellular carcinoma (HCC) tissues compared to normal liver tissues, with this finding being consistent across the Chen Liver and Roessler Liver 2 datasets. The difference was statistically significant with $***P < 0.001$. **B.** Kaplan-Meier survival curves were used to compare the prognostic significance of B4GALT1 expression in patients with HCC, using KM plotter and R2 web tools. Patients were divided into groups based on low or high expression levels of B4GALT1 in HCC. Survival differences were determined using the log-rank test. **C.** B4GALT1 expression levels were assessed and quantified through immunohistochemistry (IHC), accompanied by a scale bar for size reference at 50 μm . **D.** Comparison of B4GALT1 expression between HCC tumors (T) and their corresponding non-tumor liver tissue (N), with "N > T" indicating higher expression in non-tumor tissue, and "N \leq T" indicating equal or lower expression in non-tumor tissue compared to the HCC tumor. Illustrative images are provided, each with a scale bar of 50 μm . **E.** Kaplan-Meier analysis was utilized to evaluate the impact of B4GALT1 expression levels on the survival of patients with

HCC, with the P value being calculated through the log-rank test. Data across studies are presented as mean values with standard deviation, with $**P < 0.01$ indicating statistical significance as per Student's t-test.



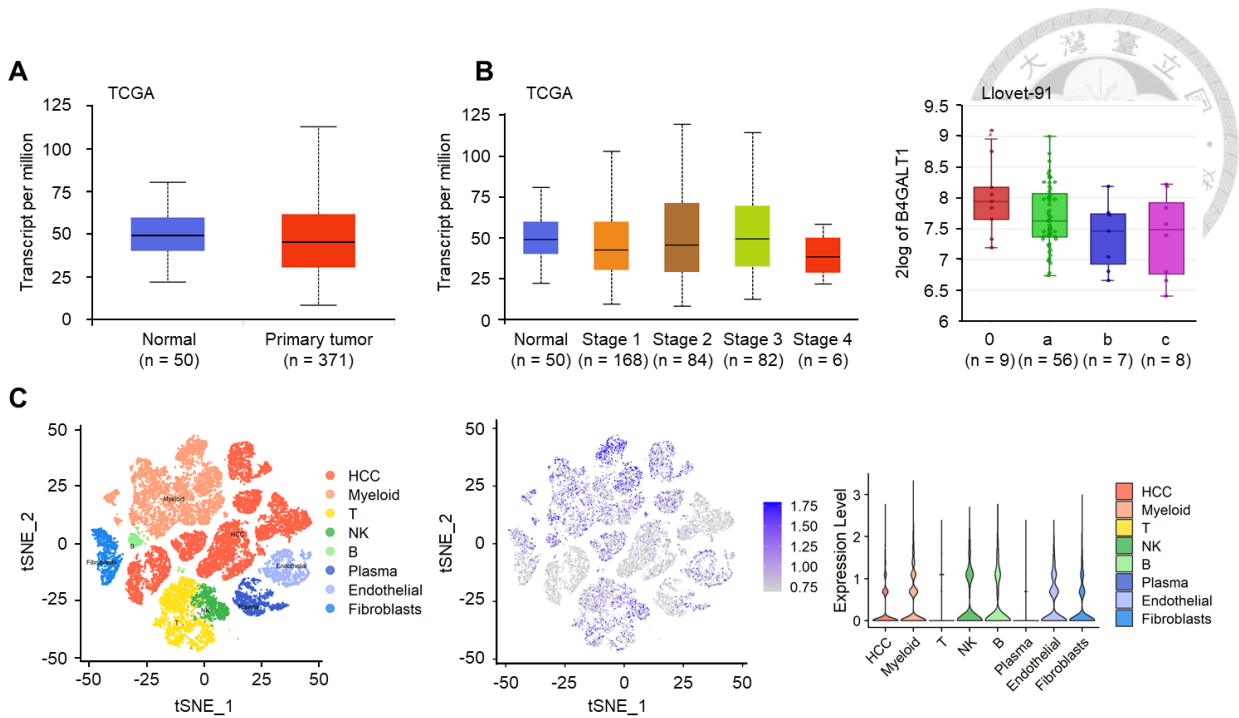


Figure 3. B4GALT1 expression in normal and HCC tissues.

A. Comparative analysis of B4GALT1 mRNA expression in normal liver versus hepatocellular carcinoma (HCC) tissues utilizing the Cancer Genome Atlas (TCGA) database, conducted through the UALCAN platform. **B.** Analysis of the relationship between B4GALT1 expression and HCC progression across two databases. The left panel details the TCGA database's clinical pathological staging for HCC (stages 1 through 4), while the right panel refers to the Llovet-91 database, which categorizes HCC according to the Barcelona Clinic Liver Cancer (BCLC) staging system (from 0 for very early stage to C for advanced stage). **C.** Single-cell RNA sequencing (scRNA-seq) profiling of B4GALT1 in both HCC and stromal cells, with dataset ID: EGAD00001006190. The left panel presents a t-distributed Stochastic Neighbor Embedding (tSNE) plot depicting eight distinct cell clusters from ten HCC tumors, each cluster denoted by a different color. The middle panel exhibits a plot of B4GALT1 expression levels across these eight cell clusters. The right panel is a violin plot illustrating the relative expression levels of B4GALT1 within the same clusters.

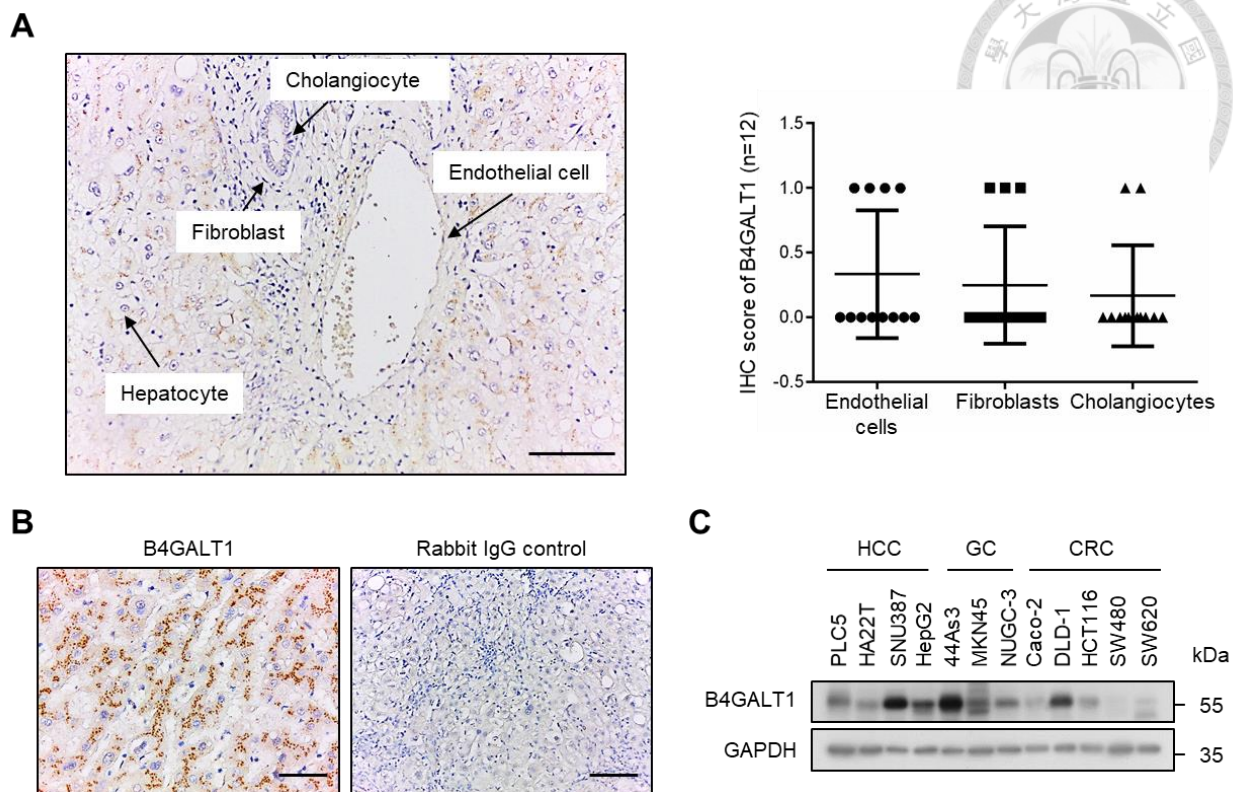


Figure 4. B4GALT1 expression in liver stromal cells and in various cancer cell lines.

A. Examination of B4GALT1 levels in various liver stromal cells, such as endothelial cells, fibroblasts, and cholangiocytes. The left panel provides an illustrative image from immunohistochemical (IHC) analysis of B4GALT1 in a healthy liver, with a 50 mm scale bar for size reference. The right panel displays an IHC score detailing B4GALT1 expression in the indicated stromal cells. **B.** Validation of the anti-B4GALT1 antibody's specificity for use in IHC. The left panel depicts B4GALT1 staining in a normal liver sample, whereas the right panel shows that rabbit IgG, which served as a negative control, did not yield any specific staining in liver tissue. A scale bar of 50 mm is present for size comparison. **C.** Western blot evaluations of B4GALT1 expression across cell lines from hepatocellular carcinoma (HCC), gastric cancer (GC), and colorectal cancer (CRC) are delineated as noted.

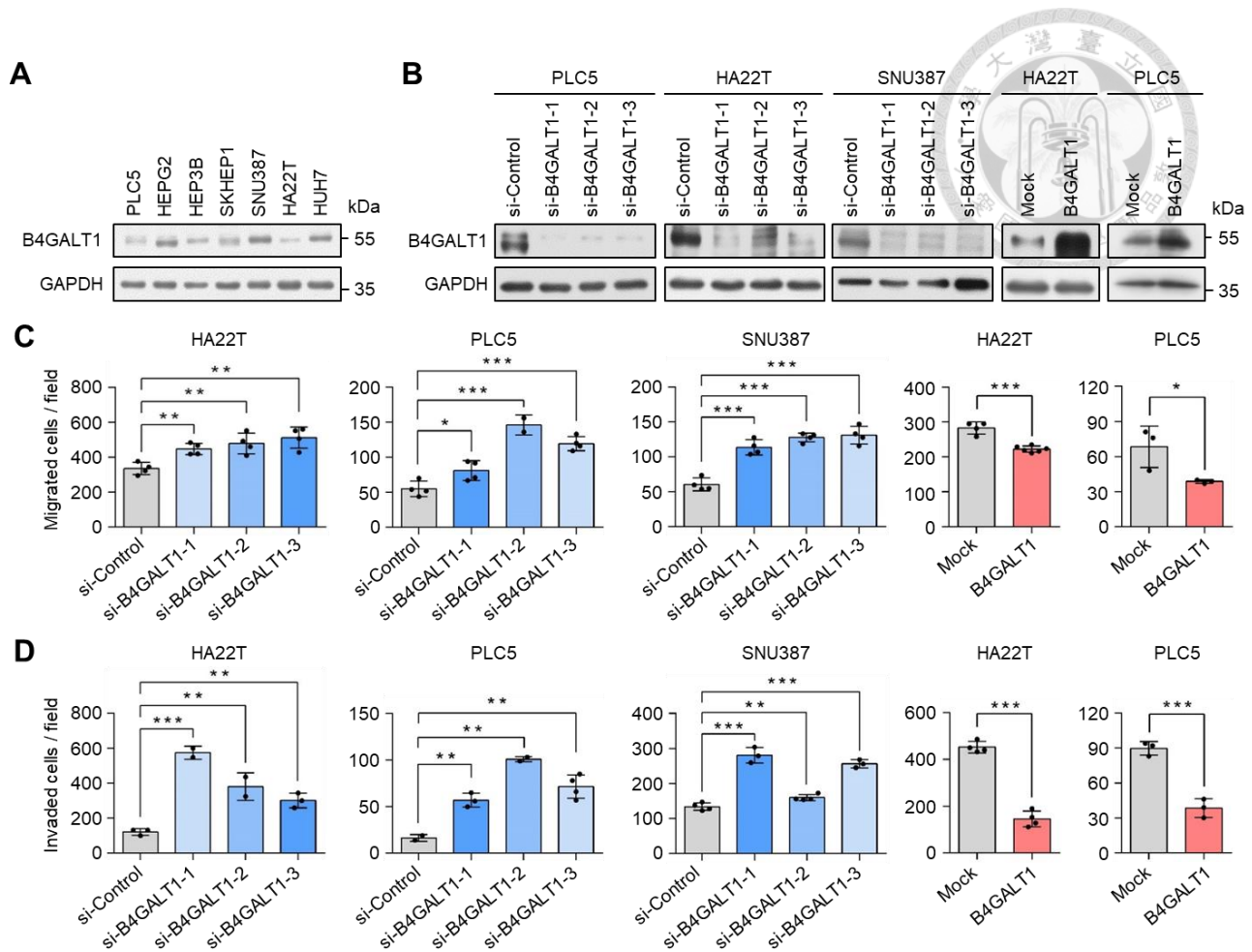


Figure 5. B4GALT1 effects of HCC cells in vitro.

A. Western blot assays illustrate the levels of B4GALT1 in various HCC cell lines. **B.** Western blot tests reveal the results of B4GALT1 suppression and heightened expression in HCC cells. Three unique B4GALT1-targeted siRNAs (si-B4GALT1-1, si-B4GALT1-2, and si-B4GALT1-3) were employed to reduce B4GALT1 in PLC5, HA22T, and SNU387 cells. A non-specific siRNA (si-Control) served as a baseline control. The B4GALT1-pcDNA3.1 plasmid was used for persistent B4GALT1 induction in PLC5 and HA22T cells, with the pcDNA3.1 vector alone (mock) as the control. **C.** The transwell migration assay was conducted to evaluate cell motility. **D.** The Matrigel invasion assay was utilized to assess the invasive properties of cells. As repeated in three independent series, the results are expressed as mean \pm standard deviation. Statistical significance was via Student's t-test as * $P < 0.05$; ** $P < 0.01$; *** $P < 0.001$.

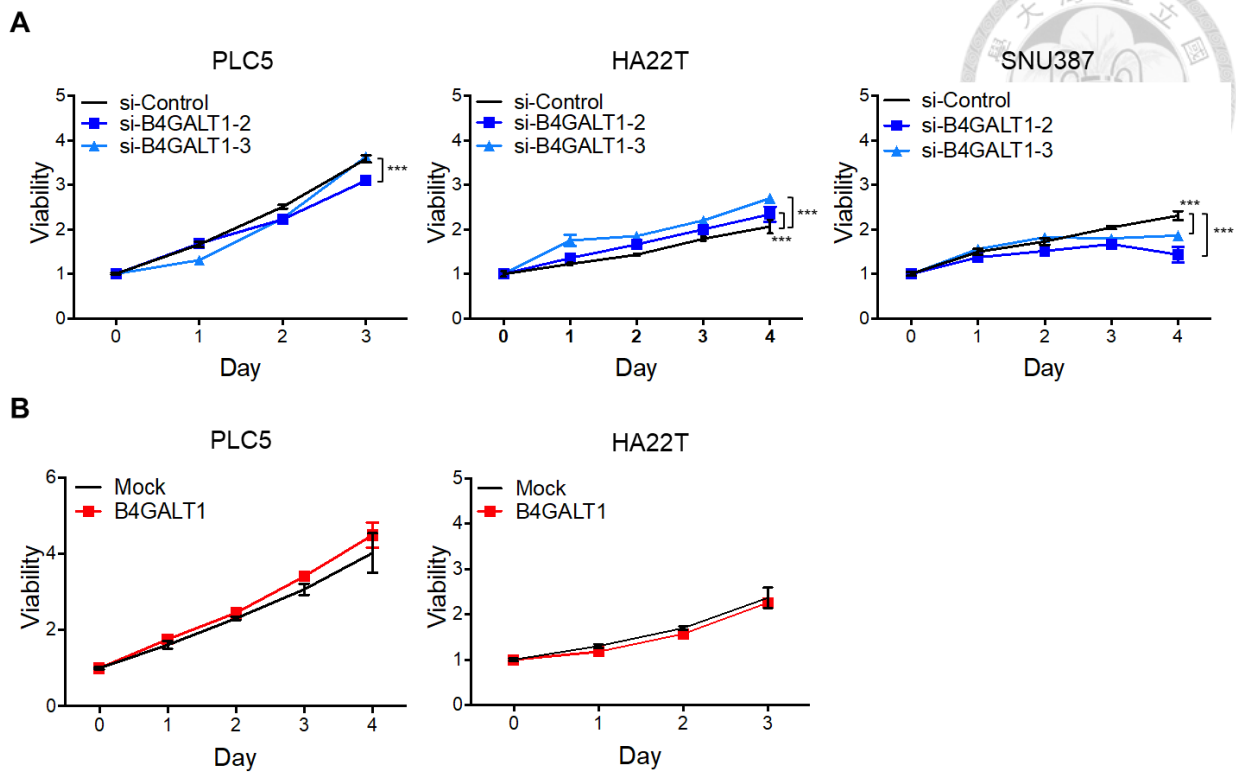


Figure 6. B4GALT1 effects on HCC cell viability.

A. The cell proliferation of diminished B4GALT1 expression on hepatocellular carcinoma (HCC) cells are detailed, with a high level of statistical significance denoted by *** $P < 0.001$ as determined by Student's t-test. **B.** The cell viability pattern of increased B4GALT1 expression on HCC cells are also noted, with the same level of statistical significance *** $P < 0.001$, established through Student's t-test.

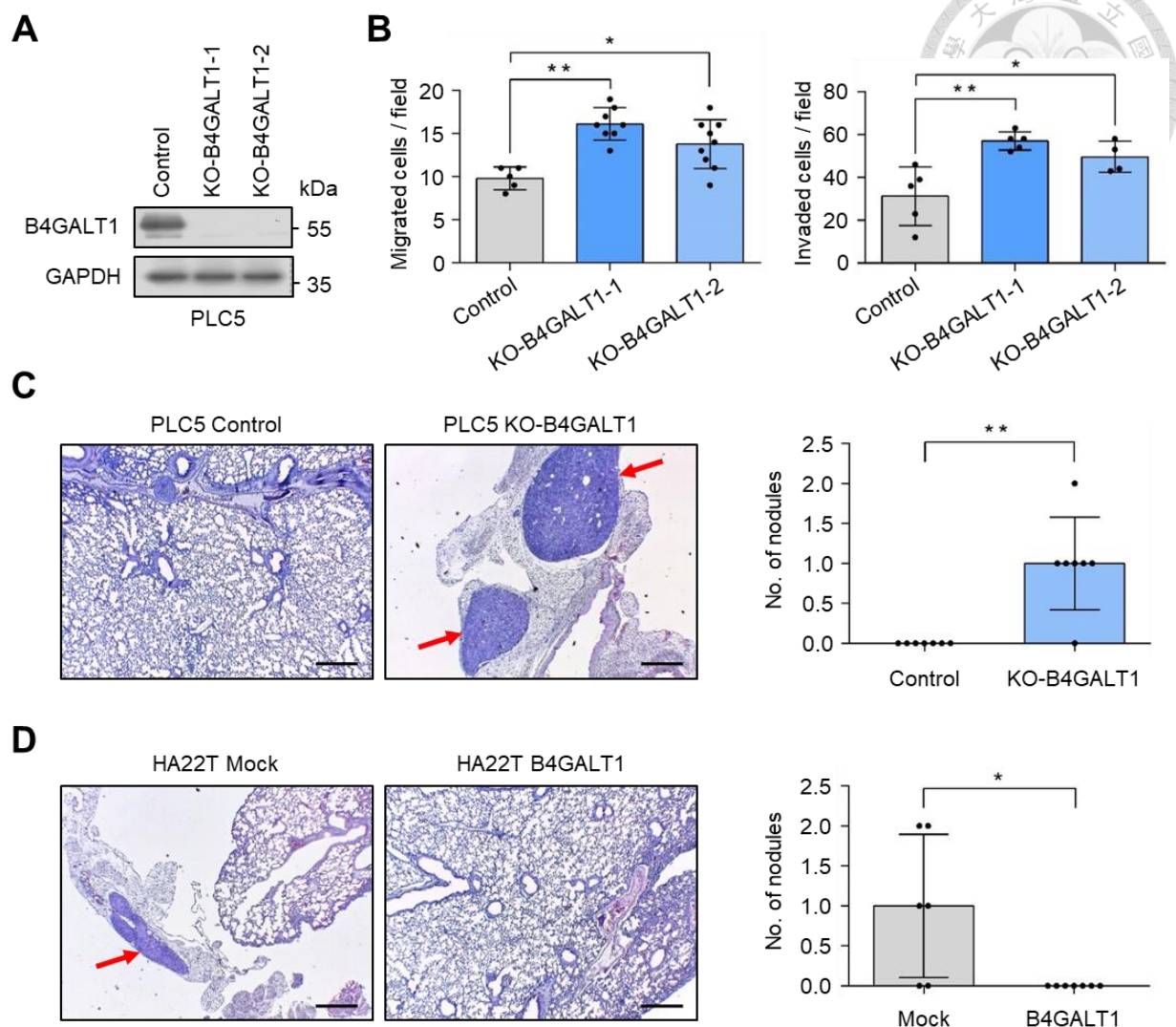


Figure 7. B4GALT1 effects on HCC cells metastasis in vivo.

A. Western blot analyses display the elimination of B4GALT1 in PLC5 cells (with clones ko-B4GALT1-1 and ko-B4GALT1-2) and its augmented expression in HA22T cells. **B.** Transwell migration and Matrigel invasion tests were employed to examine the influence of B4GALT1 absence on the motility and invasive capacity of PLC5 cells, with findings from three separate studies provided. **C.** The impact of B4GALT1 deficiency on metastatic spread is shown via images of lung metastases from original and B4GALT1-lacking PLC5 cells, where arrows mark the cancerous nodules. A 500 μ m scale is included for reference. NOD/SCID mice (seven per group) were administered PLC5 cells intravenously and were later euthanized after 60 days for lung

examination. **D.** Illustrative images depict lung metastases in liver cancer, comparing control HA22T cells to those with B4GALT1 overexpression. The group size was seven each, except for one casualty in the control cohort during the study period. Results are summarized as average values with standard deviation. Statistical significance was appraised using Student's t-test, with *P < 0.05; **P < 0.01 indicating the level of significance.

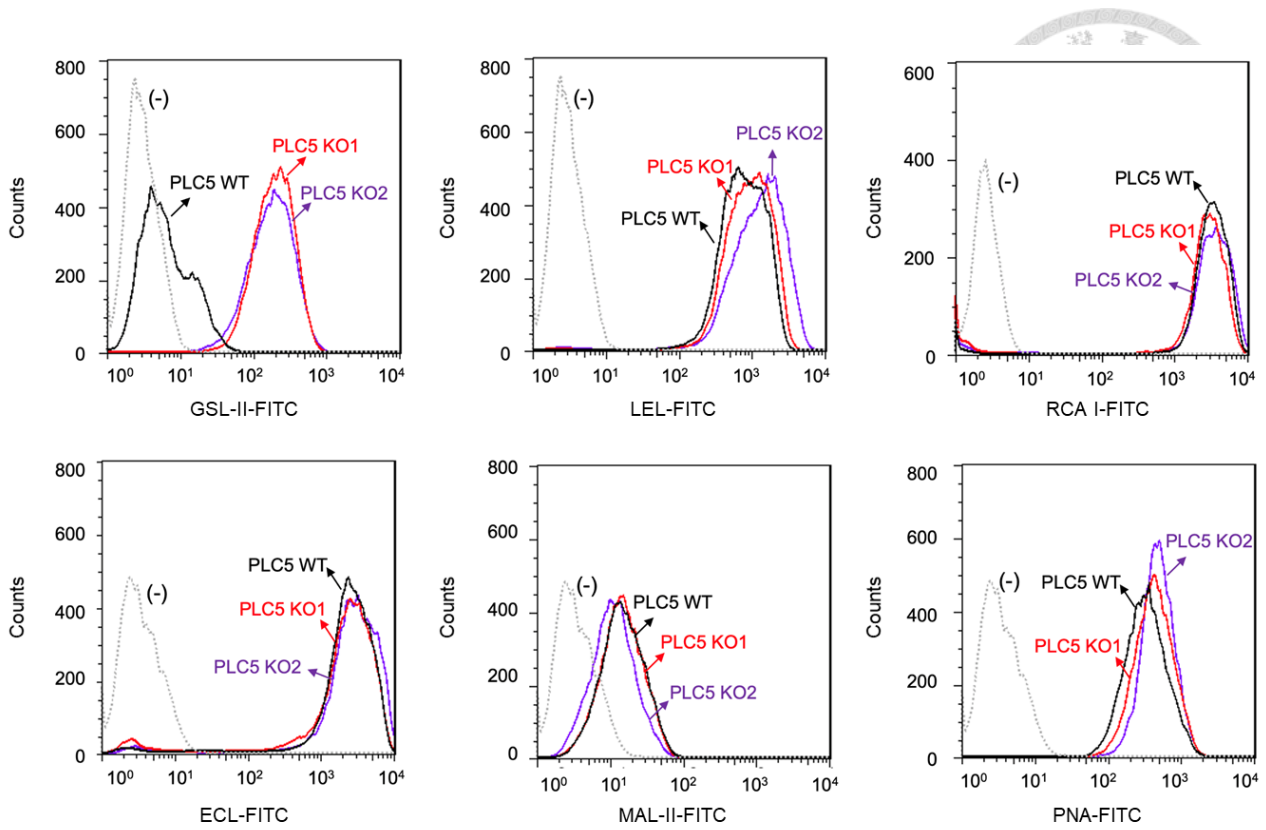


Figure 8. Effects of B4GALT1 knockout on glycophenotypes in PLC5 cells.

The surface glycan profiles of PLC5 cells, both wild-type and B4GALT1-deficient (with two distinct knockout clones labeled KO1 and KO2), were characterized through flow cytometry employing fluorescein isothiocyanate (FITC)-tagged lectins as specified.

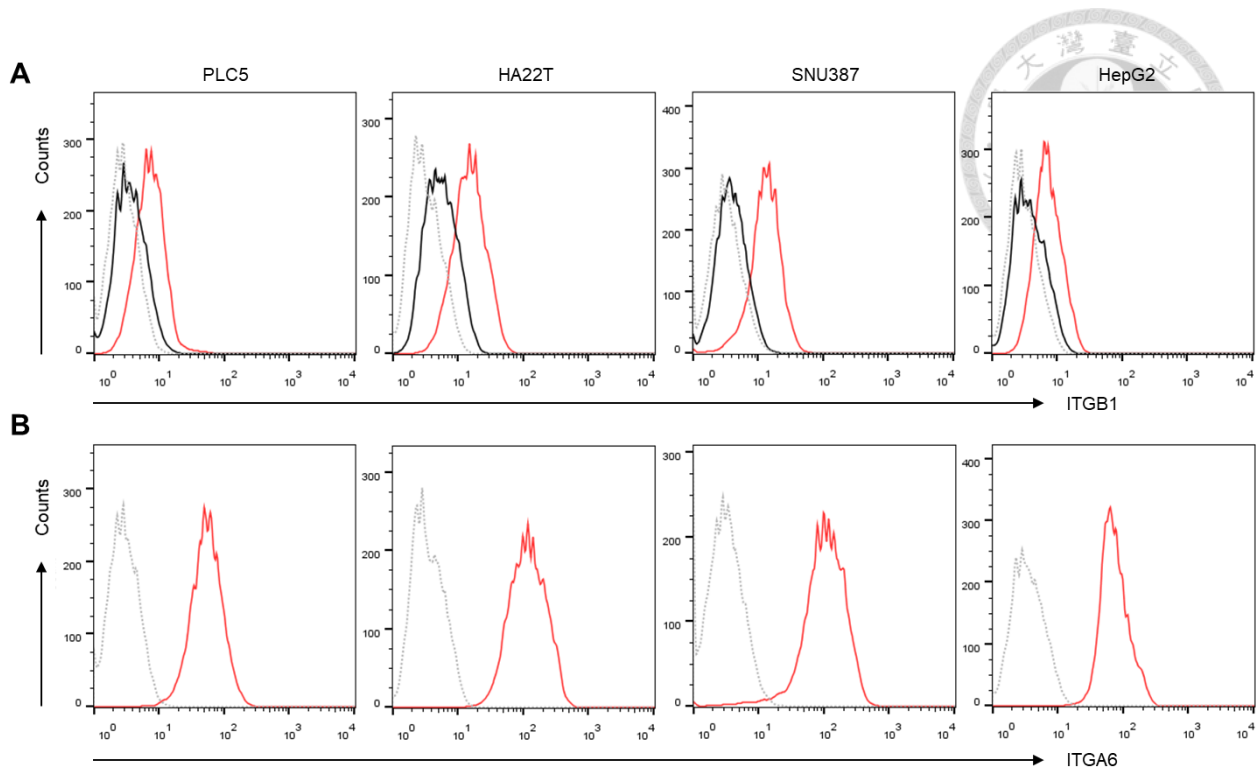


Figure 9. Flow cytometric analysis of ITGB1 and ITGA6 expression on the cell surface of HCC cells.

A. Flow cytometric analysis for ITGB1 in hepatocellular carcinoma (HCC) cells as marked. **B.**

Flow cytometric assessment for ITGA6. The dotted lines represent the cells tagged with corresponding primary antibodies. Cells delineated by the black solid lines were stained solely with a FITC-labeled secondary antibody. Red lines showcase cells that were stained using an integrin-specific antibody. The anti-ITGB1 antibody used was an unmodified, purified form. Conversely, the anti-ITGA6 antibody was tagged with phycoerythrin (PE) conjugation.

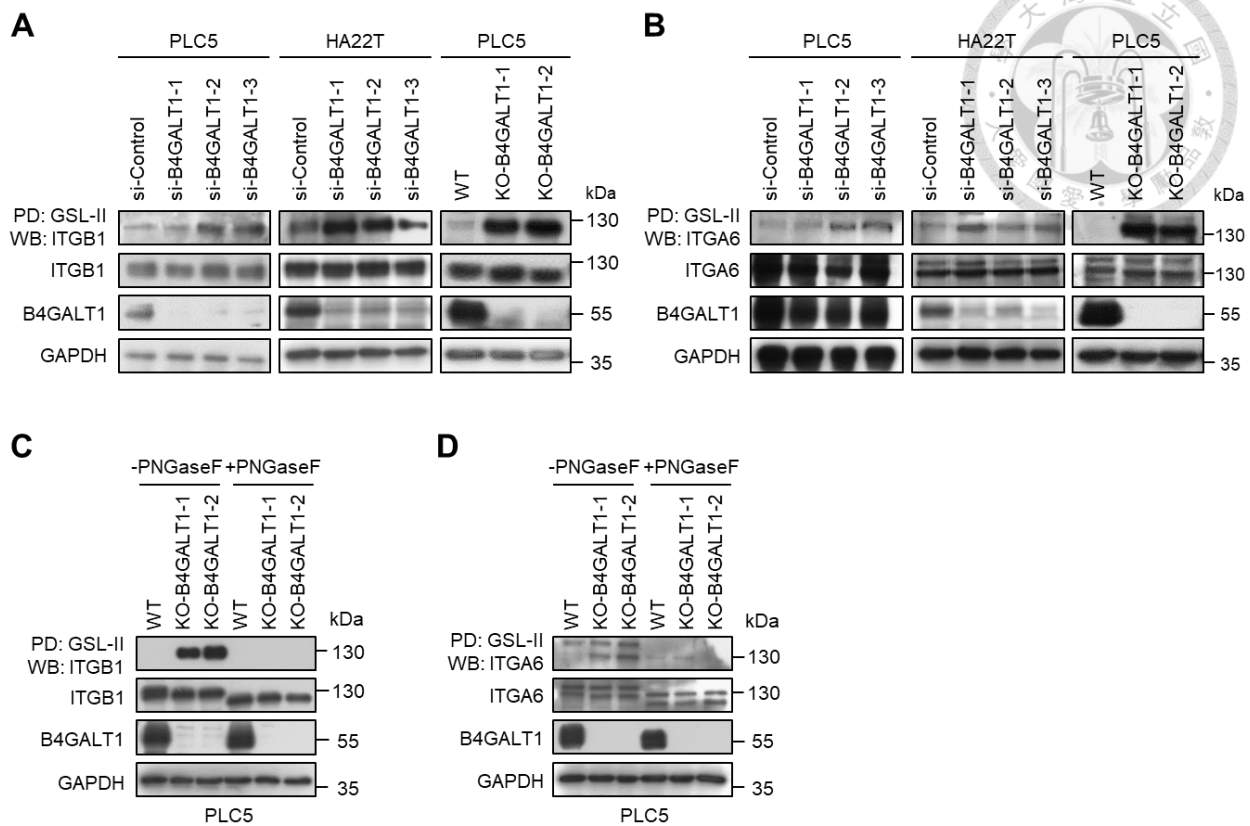
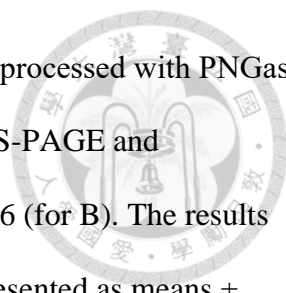


Figure 10. The role of B4GALT1 in HCC cells in overseeing the process of integrins $\alpha 6$ and $\beta 1$ glycosylation.

A. Griffinia simplicifolia lectin II (GSL-II) bead capture assay targeting integrin $\beta 1$. Proteomic extracts from PLC5 and HA22T cells with reduced B4GALT1 expression and B4GALT1-null PLC5 cells underwent affinity capture using GSL-II agarose beads and were subsequently probed with anti-integrin $\beta 1$ (ITGB1) antibodies. Three distinct B4GALT1 siRNAs and two separate B4GALT1 knockout clones were incorporated as specified. **B.** GSL-II bead affinity assay for integrin $\alpha 6$. Cellular proteins from PLC5 and HA22T cells with B4GALT1 knockdown and B4GALT1-null PLC5 cells were isolated with GSL-II agarose beads and then subject to immunoblotting with antibodies against integrin $\alpha 6$ (ITGA6). **C.** B4GALT1's primary role in the modification of N-glycans on integrin $\beta 1$. Lysates from PLC5 cells were enzymatically treated with PNGase F, captured using GSL-II lectin, and the associated proteins were resolved by 6% SDS-PAGE for immunoblotting analysis with anti-ITGB1 antibodies. **D.** Predominant alteration of



N-glycans on integrin $\alpha 6$ by B4GALT1. Similarly, PLC5 cell lysates were processed with PNGase F, isolated using GSL-II lectin, with the proteins then separated on 6% SDS-PAGE and immunoblotted using antibodies directed against ITGA6 (for A) and ITGA6 (for B). The results presented are culled from three individual experiments, and the data are presented as means \pm standard deviation. Statistical significance was determined by Student's t-test, with *P < 0.05; **P < 0.01; ***P < 0.001 indicating levels of significance.

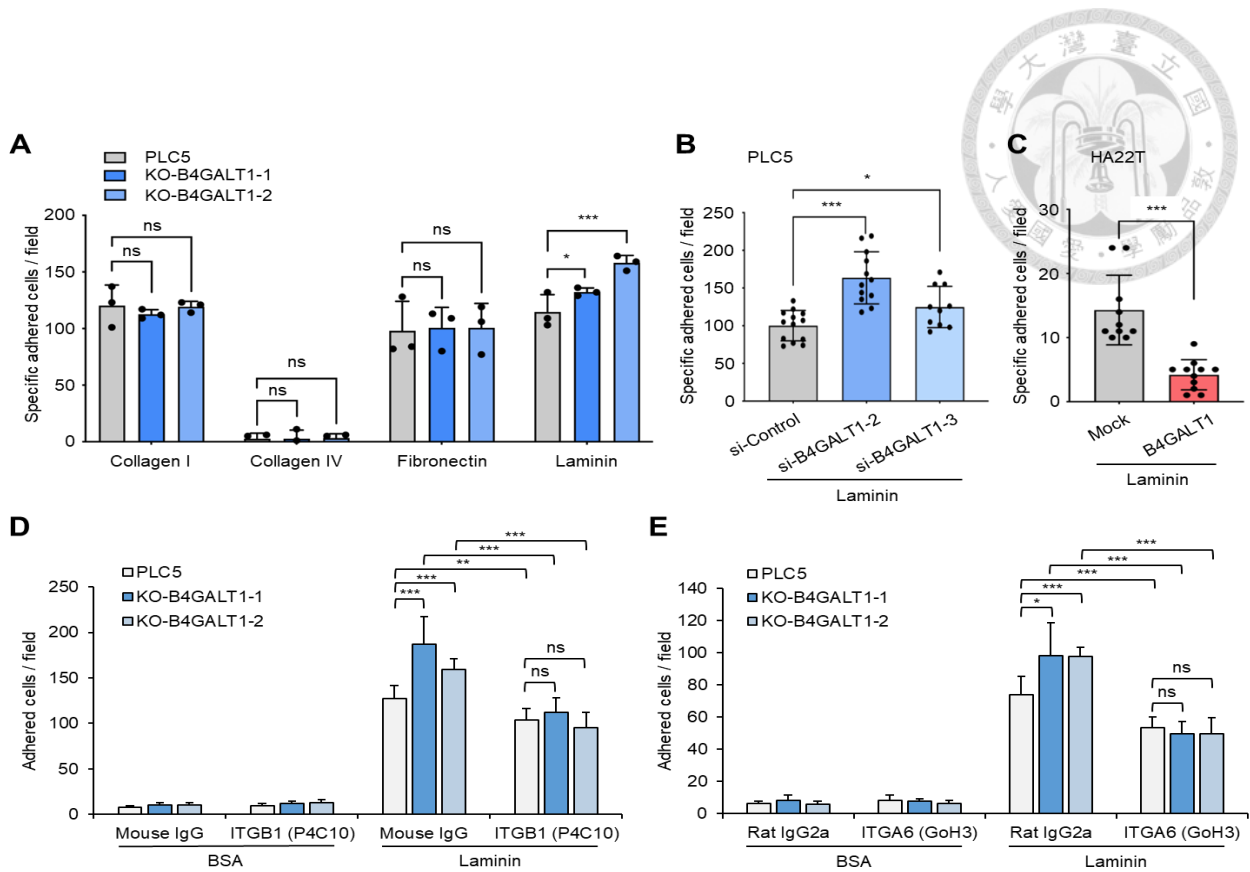


Figure 11. B4GALT1 exerts influence over the adhesion of HCC cells to laminin.

A. Studying the impact of B4GALT1 deletion on cell adherence to the extracellular matrix (ECM), PLC5 cells with or without B4GALT1 (utilizing two clones: ko-B4GALT1-1 and ko-B4GALT1-2) were distributed into wells coated with various ECM proteins including collagen I, collagen IV, fibronectin, and laminin. Post a 30-minute incubation, wells were rinsed thrice with PBS, and adherent cells were tallied using an inverted microscope. Data represent averages from three independent trials, with the specific number of adherent cells calculated by subtracting the count on BSA from that on ECM proteins. **B.** Investigating the influence of elevated B4GALT1 levels on cell adhesion to laminin, HA22T cells, either with mock treatment or with induced B4GALT1 overexpression, were seeded onto laminin-coated wells. **C.** Analyzing the consequence of B4GALT1 downregulation on adhesion to laminin, PLC5 cells were either left unaltered or subjected to B4GALT1 knockdown, and then seeded onto laminin-coated wells using two separate siRNAs (si-B4GALT1-2 and si-B4GALT1-3). **D.** Wild-type or B4GALT1-deficient PLC5 cells

were pre-treated with an integrin β 1 inhibitory antibody (P4C10) or a control mouse IgG for 10 minutes before being placed in laminin-covered wells for half an hour. **E.** PLC5 cells, both wild-type and B4GALT1-deficient, were exposed to an integrin α 6 blocking antibody (GoH3) for 10 minutes prior to being allocated into wells with a laminin base for 30 minutes. Rat IgG2a served as the control. For all tests, results are given as mean \pm standard deviation. Significance was evaluated using the Student's t-test, with p-values *P < 0.05; **P < 0.01; ***P < 0.001; ns denoting non-significance.

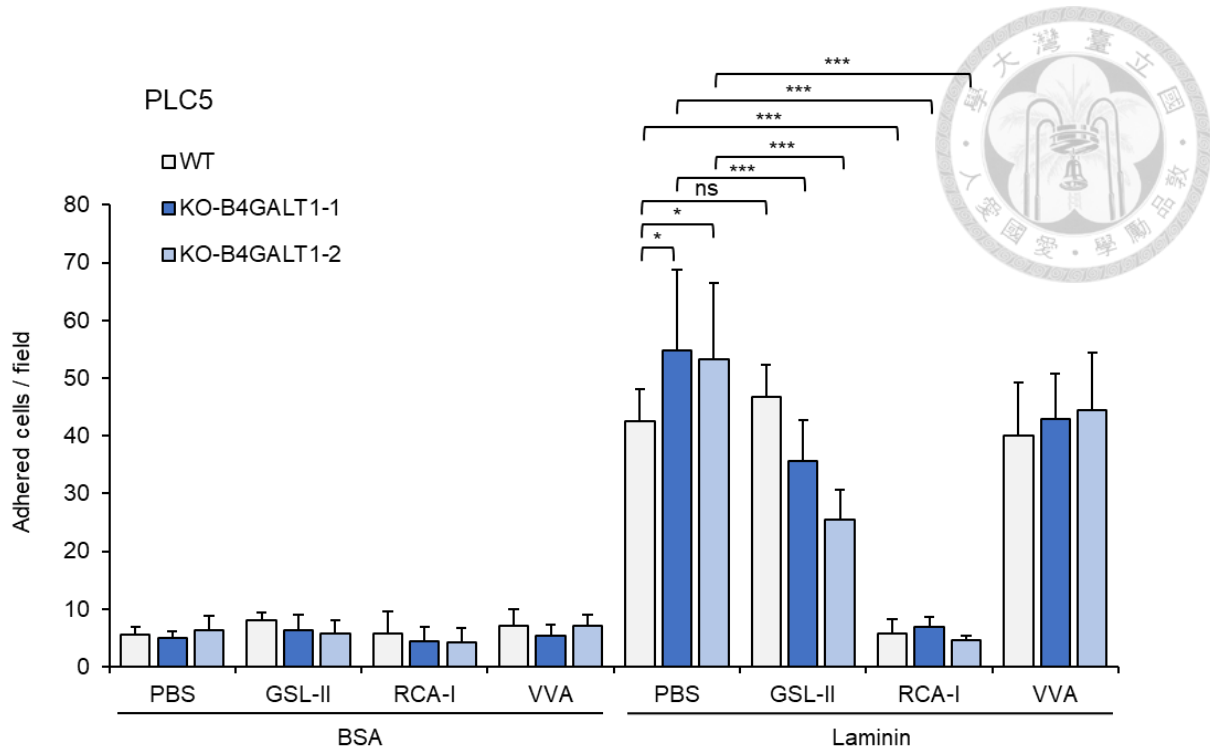


Figure 12. Effects of GSL II, RCA I, and VVA lectin on cell-laminin adhesion.

PLC5 cells, both wild-type and with B4GALT1 gene knockout, were treated with a range of lectins for a brief pre-incubation period of 10 minutes, and then the cells were placed onto plates coated with laminin and left to adhere for 30 minutes at 4°C. The number of cells that successfully adhered was quantified using microscopic examination. Bovine serum albumin (BSA) served as the control, representing a non-extracellular matrix (non-ECM) protein. The findings are presented as average counts \pm standard deviation, with statistical annotations: * $P < 0.05$; *** $P < 0.001$; ns indicating statistical non-significance.

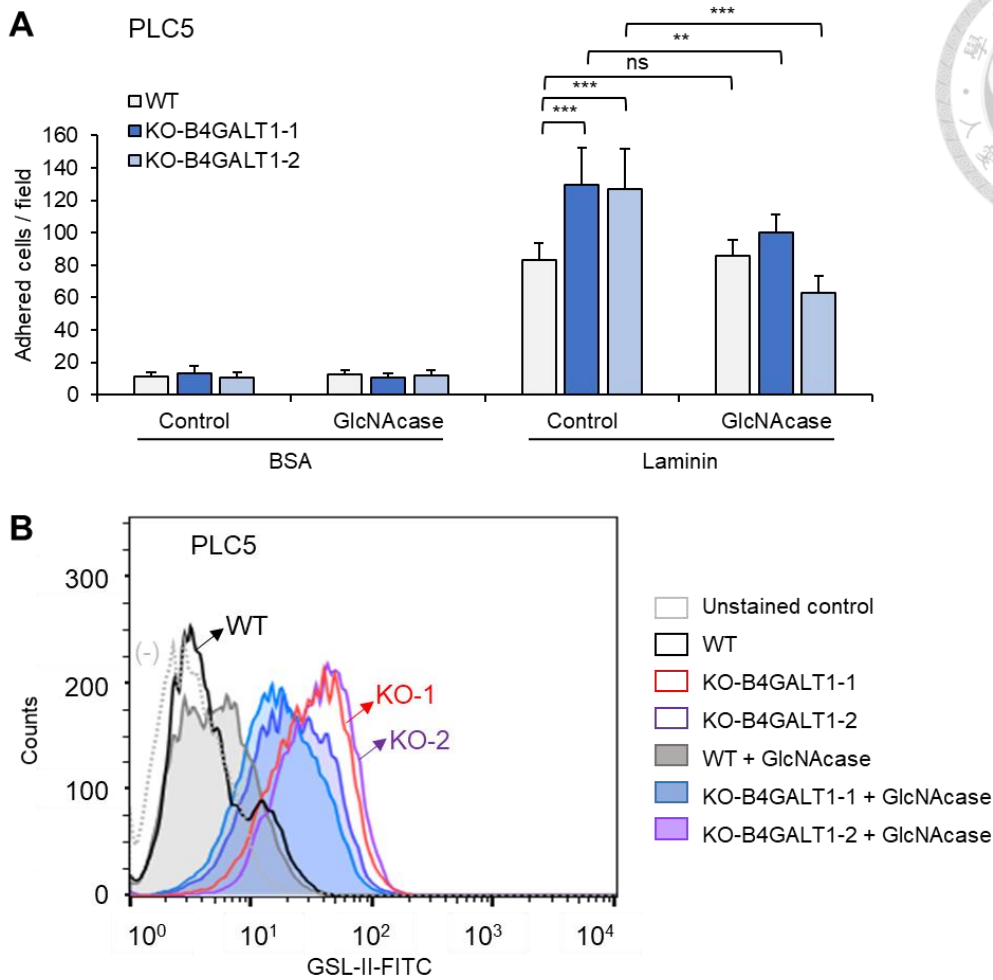


Figure 13. Effects of N-acetylglucosaminidase on cell-laminin adhesion and GSL II binding.

A. Evaluating the effect of N-acetylglucosaminidase (GlcNAcase) on the adhesion of cells to laminin. PLC5 cells, either in their wild-type form or with B4GALT1 gene disruption, were incubated with GlcNAcase or a PBS buffer as a control for 30 minutes before being placed in laminin-prepped 96-well plates for the same duration. Bovine serum albumin (BSA) was utilized as a negative control. The data are reported as mean values \pm standard deviation. Statistical significance was assessed with ** $P < 0.01$; *** $P < 0.001$; ns indicating a lack of significant difference. **B.** Wild-type (WT) and B4GALT1 knockout (KO) cell lines underwent GlcNAcase treatment followed by an evaluation of Griffonia simplicifolia lectin II (GSL II) binding through flow cytometry analysis.

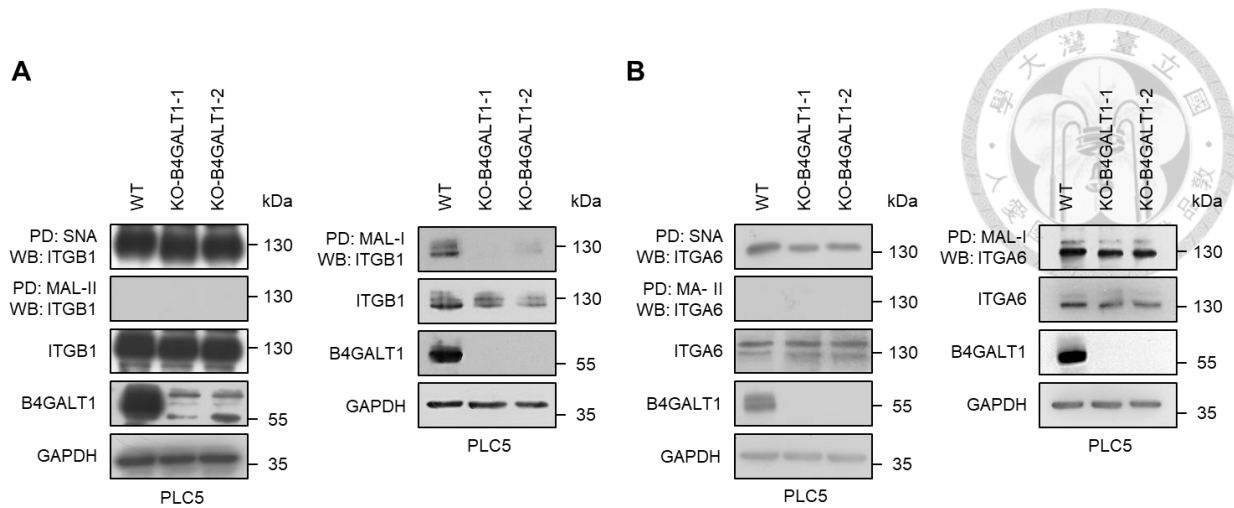


Figure 14. The sialylation patterns within ITGB1 and ITGA6 in PLC5 cells following the knockout of B4GALT1.

A. Lectin affinity assay targeting ITGB1. **B.** Lectin affinity assay focusing on ITGA6. Proteins from wild-type or B4GALT1-deficient PLC5 cells were isolated using Sambucus nigra agglutinin (SNA), Maackia amurensis lectin I (MAL I), or Maackia amurensis lectin II (MAL II), followed by Western blot analysis to detect integrins.

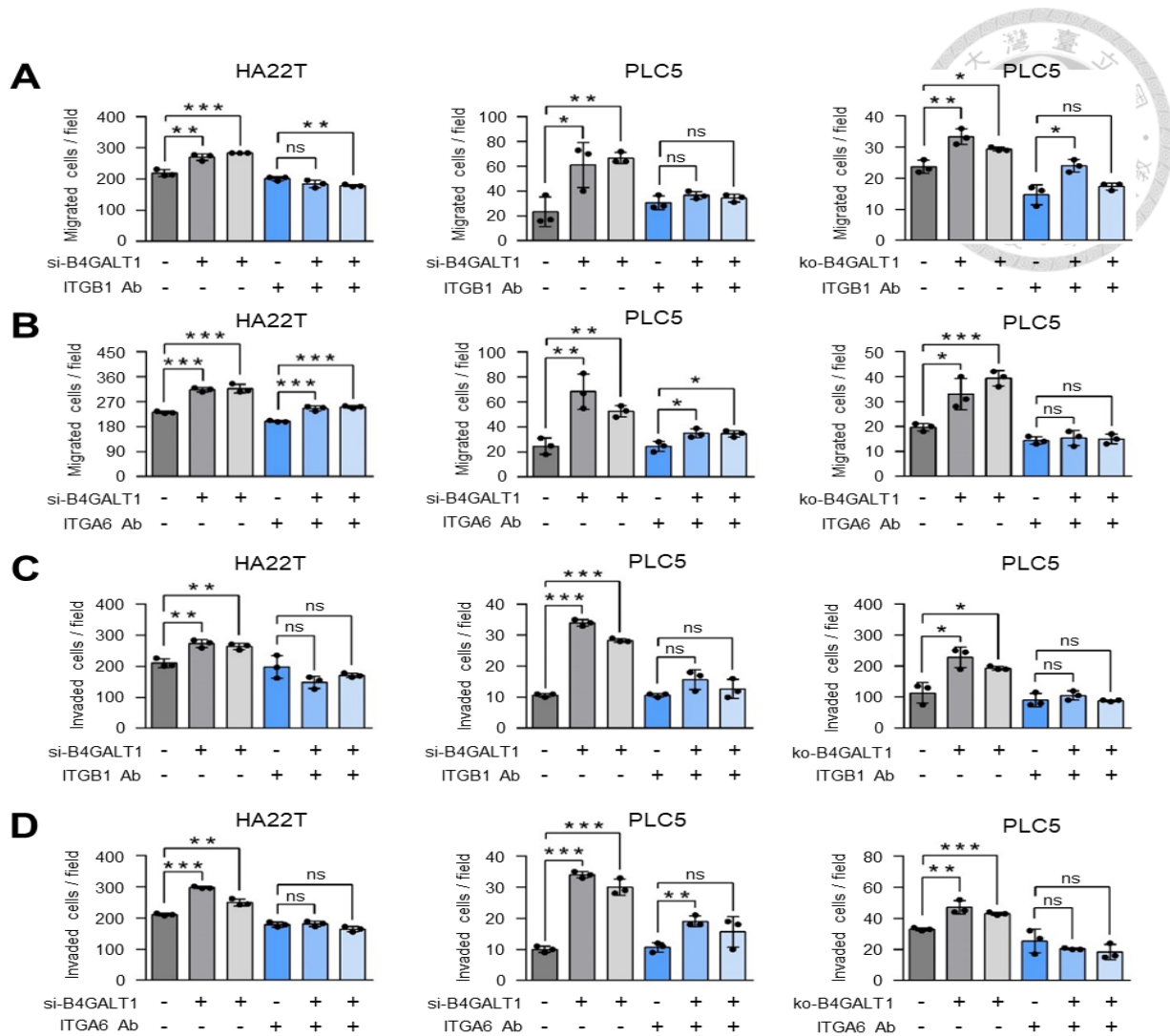


Figure 15. Blockade of integrin $\beta 1$ or integrin $\alpha 6$ impedes the migration and invasion promoted by B4GALT1 knockdown or knockout in HCC cells.

A. Transwell assays indicate that the mobility of HA22T and PLC5 cells, enhanced by B4GALT1 siRNA treatment or B4GALT1 gene deletion, was notably inhibited in the presence of an anti-integrin $\beta 1$ (ITGB1) antibody. Two distinct B4GALT1-targeting siRNAs and a non-specific control siRNA were applied to both HA22T and PLC5 cell lines. Additionally, two separate B4GALT1-deficient PLC5 cell clones along with the unaltered PLC5 cells were analyzed. Mouse IgG served as a baseline control. **B.** Transwell assays reveal that the anti-integrin $\alpha 6$ (ITGA6) antibody substantially reduced the B4GALT1 siRNA-mediated or gene deletion-induced heightened cell migration in both HA22T and PLC5 cells. **C.** Matrigel invasion tests demonstrate the

suppressive effect of the anti-integrin $\beta 1$ antibody on the increased invasive behavior of HA22T and PLC5 cells subject to B4GALT1 siRNA interference or gene knockout. **D.** Matrigel invasion assays elucidate the role of anti-integrin $\alpha 6$ antibody in curtailing the augmented invasion capacity of HA22T and PLC5 cells mediated by B4GALT1 siRNA or knockout. The displayed results are from three separate experiments, with data expressed as mean \pm standard deviation. Significance levels were determined by Student's t-test with *P < 0.05; **P < 0.01; ***P < 0.001 denoting statistical relevance.

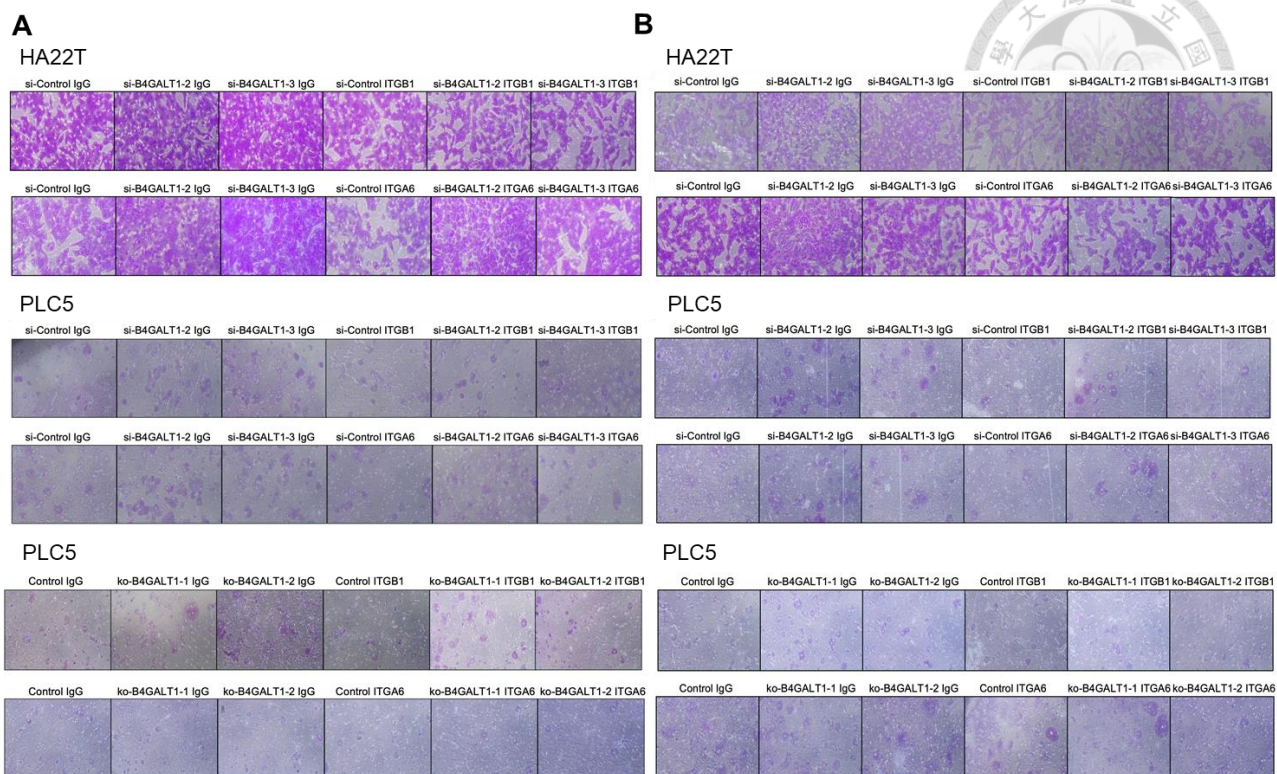


Figure 16. Representative images of HCC cell migration and invasion blocked with an anti-integrin $\beta 1$ or anti-integrin $\alpha 6$ antibody.

A. The translocation of cells was evaluated through transwell migration experiments. **B.** The infiltrative potential of cells was assessed by Matrigel invasion procedures. Independent siRNAs (si-B4GALT1-2, and si-B4GALT1-3) were utilized to diminish B4GALT1 expression in HA22T and PLC5 cells, as denoted. For the complete removal of B4GALT1 in PLC5 cells, two distinct clones (ko-B4GALT1-1 and ko-B4GALT1-2) were employed, as specified. In the upper compartment, antibodies targeting integrin $\beta 1$ (ITGB1), integrin $\alpha 6$ (ITGA6), or a control IgG were introduced as noted.

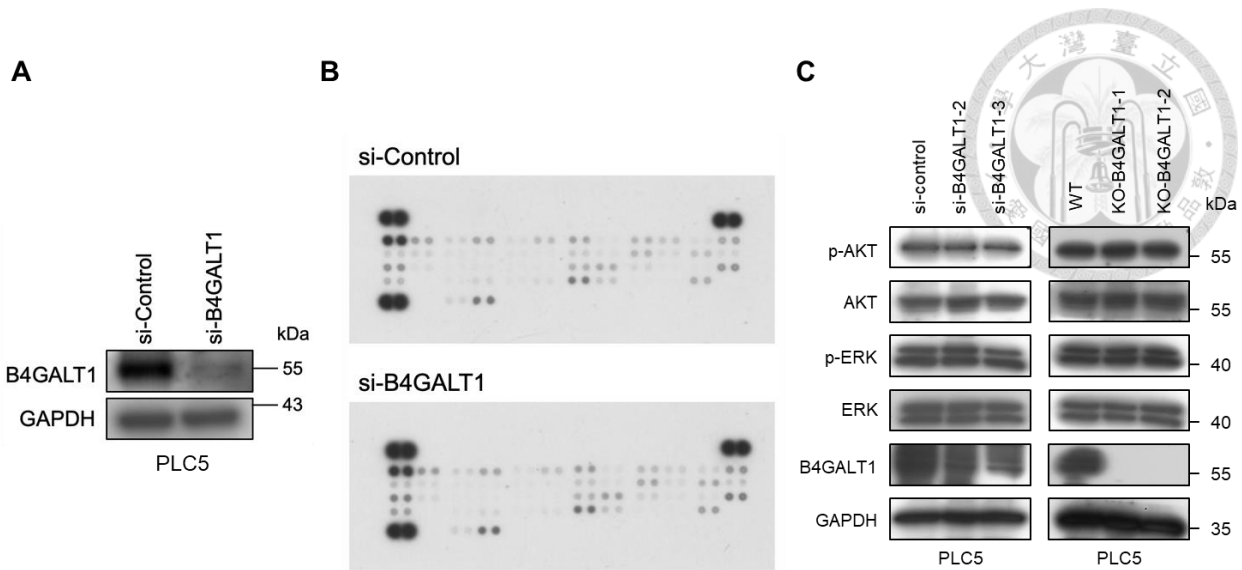


Figure 17. B4GALT1 knockdown does not significantly change levels of phospho-RTKs.

A. Western blot assays demonstrate the reduction of B4GALT1 expression in PLC5 cells post siRNA treatment. GAPDH serves as a housekeeping protein for comparison. **B.** Analysis of phospho-receptor tyrosine kinase array in PLC5 cells after silencing B4GALT1 compared to cells treated with a control siRNA. **C.** Western blot analyses reveal the impact of B4GALT1 suppression or complete elimination on the phosphorylation status of AKT and ERK in PLC5 cells.

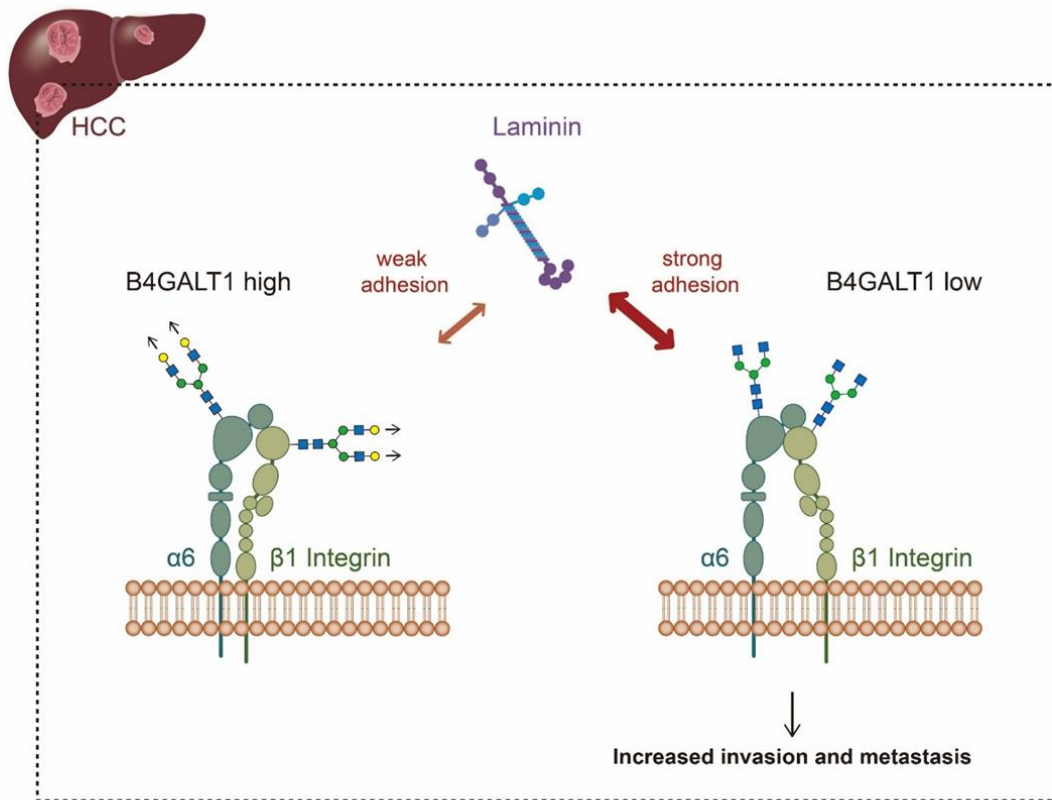


Figure 18. A diagrammatic illustration portraying the conceptualized mechanism by which B4GALT1 regulates HCC invasiveness.

The reduction of B4GALT1 leads to heightened invasive tendencies in HCC by modifying the N-glycosylation process and the role of the laminin receptor, integrin $\alpha6\beta1$.



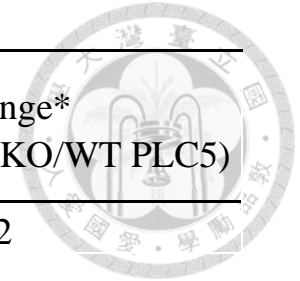
Table 1. Correlation of B4GALT1 intensity and clinicopathologic features.

	High expression (n = 28)	Low expression (n = 50)	<i>P</i> value
Sex Male:Female	20:8	27:23	0.569
Cirrhosis	12	17	0.656
Tumor size (cm ³)	83.6 (2-638)	178.1 (2-1320)	0.172
Encapsuled	12	25	0.303
Vascular invasion	4	24	0.004**
Metastasis	1	1	0.281
Differentiation grade (1:2:3:4)	1:12:14:1	0:25:23:2	0.365
TNM Staging(I:II:III:IV)	19:4:4:1	21:19:9:2	0.217
Recurrence	10	14	0.412
Overall survival (months)	70.4 (15-125)	54.9 (5-125)	0.032*

P* < 0.05; *P* < 0.01

Table 2. Glycoproteomic analysis reveals potential substrates of B4GALT1 in PLC5 cells

Rank	Gene	Accession	Protein name	MW [kDa]	calc. pI	Mascot score	Fold change* (GSL-II pulldown, KO/WT PLC5)
1	ITGB1	P05556	Integrin beta-1	88.4	5.39	534	24.52
2	SLC1A5	Q15758	Neutral amino acid transporter B(0)	56.6	5.48	170	9.84
3	ITGA6	P23229	Integrin alpha-6	126.5	6.61	39	8.26
4	CP	P00450	Ceruloplasmin	122.1	5.72	155	7.43
5	SLC39A14	Q15043	Zinc transporter ZIP14	54.2	5.33	38	5.76
6	LGALS3BP	Q08380	Galectin-3-binding protein	65.3	5.27	858	4.58
7	INSR	P06213	Insulin receptor	156.2	6.2	246	3.41
8	GDF15	Q99988	Growth/differentiation factor 15	34.1	9.66	207	2.65
9	KDEL2	P33947	ER lumen protein-retaining receptor 2	24.4	8.72	92	2.11
10	KDEL1	P24390	ER lumen protein-retaining receptor 1	24.5	8.62	94	2.00



* Only proteins with fold change ≥ 2 in the secretory pathway are listed. KO, B4GALT1 knockout; WT, wild type.